DNA 4411F

AN INVESTIGATION OF THE VALIDITY OF APPLYING MIL-STD-285 TO EMP SHIELDING EFFECTIVENESS

(12)

Harris Corporation
Electronic Systems Division
P.O. Box 37
Melbourne, Florida 32901

15 April 1977

Final Report for Period 1 October 1976—15 April 1977

CONTRACT No. DNA 001-76-C-0406

APPROVED FOR PUBLIC RELEASE;
DISTRIBUTION UNLIMITED.

THIS WORK SPONSORED BY THE DEFENSE NUCLEAR AGENCY
UNDER RDT&E RMSS CODE B32307T464 R99QAXEB09962 H25900.

Prepared for
Director
DEFENSE NUCLEAR AGENCY
Washington, D. C. 20305

Destroy this report when it is no longer needed. Do not return to sender.

UNCLASSIFIED

SECURITY CLASSIFICATION OF THIS PAGE (When Data Entered)

REPORT DOCUMENTATION PAGE

READ INSTRUCTIONS BEFORE COMPLETING FORM

1. REPORT NUMBER: DNA 4411F
2. GOVT ACCESSION NO.
3. RECIPIENT'S CATALOG NUMBER

4. TITLE (and Subtitle): AN INVESTIGATION OF THE VALIDITY OF APPLYING MIL-STD-285 TO EMP SHIELDING EFFECTIVENESS,
5. TYPE OF REPORT & PERIOD COVERED: Final Report, for Period 1 Oct 76—15 Apr 77
6. PERFORMING ORG. REPORT NUMBER

7. AUTHOR(s): Eduardo Villaseca, William Blackwood, Carl Davis, William Getson
8. CONTRACT OR GRANT NUMBER(s): DNA 001-76-C-0406

9. PERFORMING ORGANIZATION NAME AND ADDRESS: Harris Corporation, Electronic Systems Division, P.O. Box 37, Melbourne, Florida 32901
10. PROGRAM ELEMENT, PROJECT, TASK AREA & WORK UNIT NUMBERS: NWED Subtask R99QAXEB099-62

11. CONTROLLING OFFICE NAME AND ADDRESS: Director, Defense Nuclear Agency, Washington, D.C. 20305
12. REPORT DATE: 15 April 1977
13. NUMBER OF PAGES: 52 (49 p.)

14. MONITORING AGENCY NAME & ADDRESS (if different from Controlling Office): DNA, SBLE (4411F, AD-E3PP 13P)
15. SECURITY CLASS (of this report): UNCLASSIFIED
15a. DECLASSIFICATION/DOWNGRADING SCHEDULE

16. DISTRIBUTION STATEMENT (of this Report)

Approved for public release; distribution unlimited.

17. DISTRIBUTION STATEMENT (of the abstract entered in Block 20, if different from Report)

18. SUPPLEMENTARY NOTES

This work sponsored by the Defense Nuclear Agency under RDT&E RMSS Code B32307T464 R99QAXEB09962 H2590D.

19. KEY WORDS (Continue on reverse side if necessary and identify by block number)

Shielding Effectiveness
MIL-STD-285
EMP
EMC
Angular Spectrum of Plane Waves

(100 Hz To 100 MHz)

(AD-771 997)

20. ABSTRACT (Continue on reverse side if necessary and identify by block number)

HDL-TR-1636 "EMP Shielding Effectiveness and MIL-STD-285" by R. L. Monroe, concludes that measurements carried out in the manner prescribed by MIL-STD-285 will give upper and lower bounds for the EMP (Plane Wave) shielding effectiveness of any metallic structure at all frequencies of interest (10^2 to 10^8 Hz). Upper and lower bounds to EMP shielding effectiveness are provided by dipole and loop antenna measurements, respectively.

DD FORM 1 JAN 73 1473 EDITION OF 1 NOV 65 IS OBSOLETE

UNCLASSIFIED

SECURITY CLASSIFICATION OF THIS PAGE (When Data Entered)

408 172

20. ABSTRACT (Continued)

We conclude that the assumptions used in HDL-TR 1636 lead to an over-simplification of the problem. A more precise treatment is, therefore, provided which correlates the magnitude of shielding effectiveness exhibited by a planar metallic sheet to these two diverse electromagnetic fields—one being generated many wavelengths from the shield and the other being generated at a fraction of a wavelength away. This technique, termed an 'Angular Spectrum of Plane Waves' makes no simplifying assumptions, but calculates the wave form in the near field of small loop and dipole antennas in the absence of the shield and converts the actual field configuration to an equivalent family of plane waves. The family of plane waves is then transmitted through the shield and shielding effectiveness is computed from considerations of the incident power and the power transmitted through the shield.

Using the plane wave spectrum concept, theoretical values of shielding effectiveness are determined for a planar structure using loop and dipole antennas located 12 inches (0.305 m) from the shield. (MIL-STD-285 procedures). These values of shielding effectiveness are then correlated with plane wave calculations (assuming the source in the far field). The difference between these two theoretical values provides a correction factor to apply to actual MIL-STD-285 test values (near field) to obtain the corresponding shielding effectiveness of the structure to a plane electromagnetic wave (source in the far field).

TABLE OF CONTENTS

LIST OF ILLUSTRATIONS

1.0 EXECUTIVE SUMMARY

At the present time there does not exist an accepted and adequate correlation between 1) the shielding effectiveness presented by electronic equipment shelters to the nuclear generated electromagnetic pulse, and 2) the methods currently being used by industry to measure this shielding effectiveness. MIL-STD-285 is being used widely by industry to measure the shielding effectiveness characteristics of electronic equipment shelters and, in many cases, the results are being used by the DOD without modification to calculate the shielding effectiveness to nuclear generated EMP. This use of MIL-STD-285 procedures has never been adequately validated or refuted.

The purpose of this effort is to investigate the validity of using MIL-STD-285 test procedures to determine the shielding effectiveness presented by an electronic equipment enclosure to a plane wave pulse.

Very little effort has been expended by the DOD in the past to validate the applicability of low level CW test procedures of the MIL-STD-285 type to EMP shielding effectiveness. One notable exception was the effort by Monroe as presented in HDL-TR-1636. In that document, the author reported that measurements carried out in the manner prescribed by MIL-STD-285 would give upper and lower bounds for the EMP (plane wave) shielding effectiveness of any metallic structure at all frequencies of interest to EMP. An expression was obtained for the difference between EMP and loop (or dipole) shielding effectiveness exhibited by the structure. A correction factor was provided to add to loop measurements and subtract from dipole measurements to estimate the shielding effectiveness to EMP. The conclusion was reached that MIL-STD-285 measurements could be used to estimate the EMP shielding effectiveness of a structure.

HDL-TR-1636 has received little emphasis in the EMP community and has not been applied to any procurement as far as the investigators could determine. Few of the personnel contacted knew of its existence and when the document was discussed, nearly all questioned whether sufficient theoretical work had been done in the area.

A careful review of HDL-TR-1636 and the underlying assumptions supported the conclusion that an independent approach unencumbered by simplifying assumptions was needed to either validate or refute its conclusions. This new approach to shielding effectiveness is based upon the work of Booker and Clemmou[7] and employs the concept of an Angular Spectrum of Plane Waves. The effort addresses the planar structure. The concept of the Angular Spectrum of Plane Waves has been used successfully for several years to calculate the far field radiation pattern of antennas from near field measurements, where "near field" usually involves a few wavelengths from the antenna. In the current work, the theory is applied to the extreme near field reactive regime, 12 inches (0.305 m) from the antenna.

In the paper by Booker and Clemmou in April 1949, it was observed that the rectangular components of the electromagnetic field on one side of a planar aperture can be represented simply and exactly by a linear combination of plane waves. It was shown that the steady-state radiation pattern and aperture function (E_{tan} in the plane of the aperture) are obtainable from each other, and finally, that those portions of the pattern lying outside of the visible region of real angles determine completely the reactive energy stored about the aperture. In the current effort, the aperture function, E_{tan}, is obtained for dipole and loop antennas in a plane 12 inches (0.305 m) from the antenna over a matrix of 4096 points in a 100 x 100 inch (2.54 x 2.54 m) aperture. The plane wave spectrum corresponding to the electromagnetic field at any point in space is related to the aperture function by the Fourier Transform and is obtained for a hypothetical plane 12 inches (0.305 m) from the antenna. This spectrum is then considered to be impinged upon the metallic shield to obtain the shielding effectiveness. (The 12 inch (0.305 m) distance is dictated by MIL-STD-285 test procedures.)

The plane wave spectrum technique shows that the value of shielding effectiveness provided by a uniform plane metallic shield to a plane wave is bounded above and below by dipole and loop measurements, respectively. This is supported in HDL-TR-1636. Correction factors are provided by the new effort to add to shielding effectiveness measurements made by loop antennas in the near field to obtain the shielding effectiveness of the structure to an incident plane wave. Similar correction factors are provided to subtract from measured values when using dipole antennas in the near field. These correction factors correlate closely with those presented in HDL-TR-1636. Thus, that portion of HDL-TR-1636 that pertains to the shielding effectiveness of a uniform conductivity plane metallic sheet is considered validated. One may question the assumption of HDL-TR-1636 in applying Schelkunoff's basic work to a different configuration than intended, but

the assumption is confirmed by the more rigorous plane wave spectrum approach. The remainder of the effort of HDL-TR-1636 pertaining to infinite conductivity shields containing faults has not been addressed by this effort, therefore, no conclusions are presented concerning the application of Schelkunoff's approach to shields with cracks, apertures, etc.

Figure 1.0-1 summarizes the results of the effort graphically. The basic graph was a shielding effectiveness specification for electronic equipment shelters provided for a recent DOD procurement. The system specification included criteria level high altitude EMP. Shielding effectiveness measurements of shelters were made at the time of acceptance from vendors in accordance with MIL-STD-285 procedures while system acceptance was based upon performance in a high level EMP simulator. Since this is a specification curve, the measured shielding effectiveness must meet or exceed the values given. Also, given this specification, the system designers were assured of a reduction of the criteria level EMP by four orders of magnitude in the mid-range of frequencies and designed the interior electronics accordingly. Another 80 dB of shielding effectiveness was added by the use of internal shield enclosures, thus reducing the interior fields by an addition four orders of magnitude. Interior power and signal cables were also placed in shielding conduit.

The significance of this theoretical effort is that although a shelter may exhibit only 70 dB of shielding effectiveness at 0.1 MHz as measured by MIL-STD-285 (12 inch (0.305 m) diameter loops at a distance of 12 inch (0.305 m) from either side of the shelter wall) the Plane Wave Spectrum calculations show that the actual shielding effectiveness to a plane wave EMP is 140 dB* - a reducation of seven orders of magnitude. Had this been realized by the system designers early in the system cycle, less expensive protective devices might have been employed inside the shelter and the cost of the weapon system reduced accordingly.

The Plane Wave Spectrum technique and the Schelkunoff technique of HDL-TR-1636 are two completely independent approaches to shielding effectiveness yet the results for a 1 mm uniform conductivity copper shield correlate to within 6 dB. These results are shown by the circles coded P, M, and E in Figure 1.0-1.

*(This assumes a linear extrapolation from low level to high level signals, i.e., no interior arcing, no magnetic saturation, and an adequate thickness of metal. These data relate to a 1mm thick uniform conductivity copper shield.)

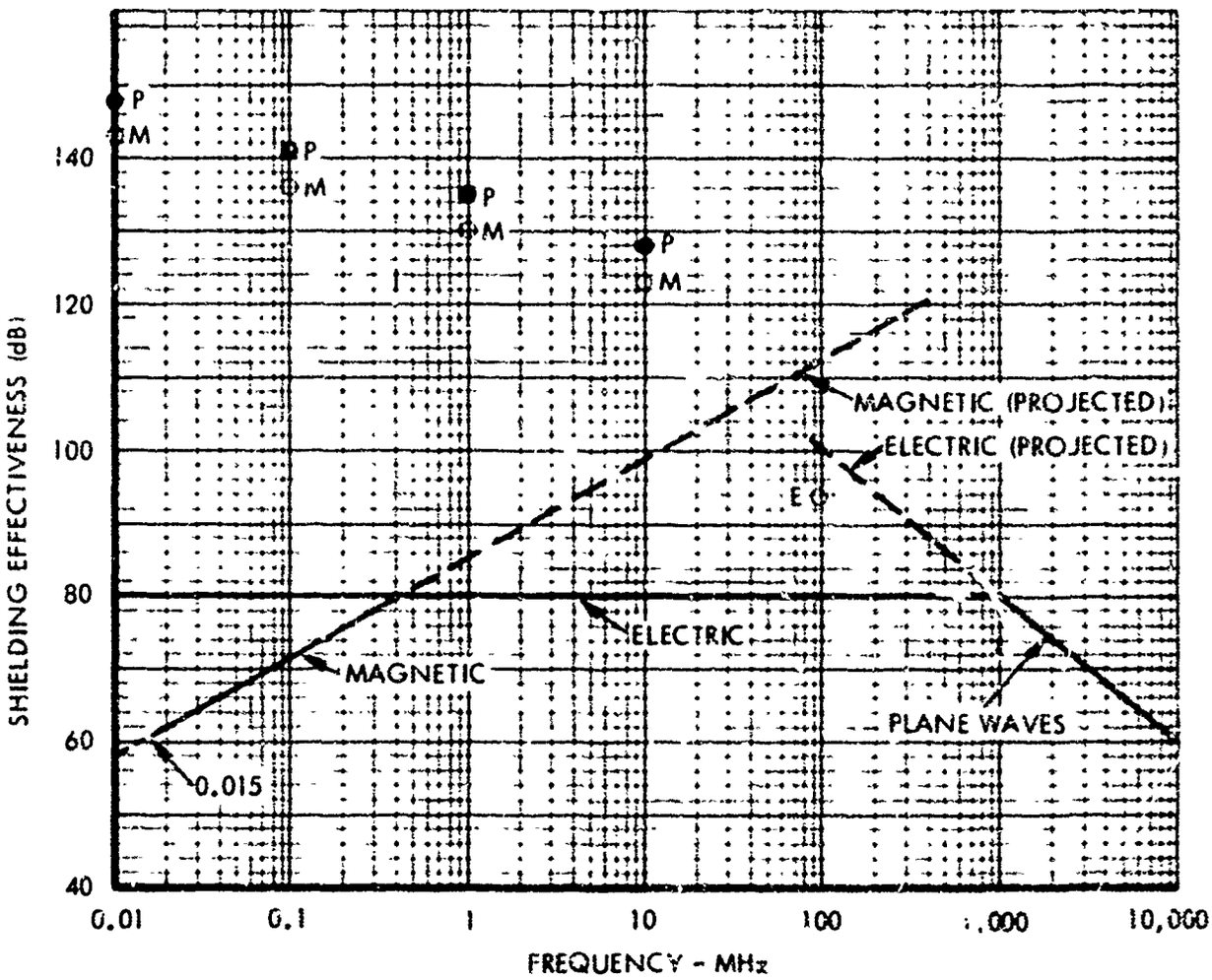

P - MAGNITUDE OF SHIELDING EFFECTIVENESS - MAGNETIC MODIFIED BY PLANE WAVE SPECTRUM DATA

M - MAGNITUDE OF SHIELDING EFFECTIVENESS - MAGNETIC - MODIFIED BY HDL-TR-1636

E - MAGNITUDE OF SHIELDING EFFECTIVENESS - ELECTRIC - MODIFIED BY HDL-TR-1636

Figure 1.0-1. Typical Shelter Shielding Effectiveness - MIL-STD-285 Specification as Modified by HDL-TR-1636 and Plane Wave Spectrum Correction Factors

2.0 PREFACE

This final technical report covers the work performed by Harris Electronic Systems Division, Melbourne, Florida, under Contract No. DNA 001-76-C-0406 for the Defense Nuclear Agency during the period October 1976 through May 1977. The program was under the direction of Dr. Carl F. Davis of the Systems Survivability Group. The effort on the Plane Wave Spectrum was under the technical direction of Mr. Eduardo Villaseca.

This contract was monitored by Captain W. D. Wilson of the Radiation Directorate of the Defense Nuclear Agency after funds had been provided by the Director of the Vulnerability Directorate, Defense Nuclear Agency.

Contributors to this effort include C. Davis, E. Villaseca, W. Getson, W. Blackwood, W. Abare, and J. Reid of Harris Electronic Systems Division and many EMI/EMP-oriented personnel throughout the DOD. We wish to express our thanks to those persons and organizations of all services who supported the effort with their time and helpful suggestions.

3.0 TECHNICAL DISCUSSION

3.1 THE PROBLEM

MIL-STD-285 specifies c method of measuring the attenuation characteristics of electromagnetic shielding enclosures used to house electronic equipment and is specifically oriented to the low-level signal problems of EMI, EMC,and TEMPEST. This Military Standard is now frequently being applied, without modification, to the measurement of shielding effectiveness of equipment shelters, weapons system bays, etc., which must provide for the survival of interior electronics to the effects of a nuclear generated electromagnetic pulse (EMP). In addition to the obvious differences in the magnitude of the signals involved in test and threat level environment, MIL-STD-285 prescribes that shielding effectiveness measurements are to be made at frequencies of interest to EMP in the near field of the radiating source, a complex wave configuration which deviates significantly from a uniform plane wave - the configuration for free field EMP.

3.2 OBJECTIVE

The objective of this effort is to investigate the applicability of low-level, MIL-STD-285, test procedures to the measurement of the shielding effectiveness of enclosures to EMP.

The Scope of Work as listed in the contract is quoted as:

> The approach used in HDL-TR-1636 will be analytically expanded and experimentally verified to provide a baseline for the application of low-level test procedures to EMP shielding effectiveness of shelters.

The approach used in HDL-TR-1636 regarding the shielding effectiveness of a planar structure without faults has been validated theoretically by the Plane Wave Spectrum calculations. The extrapolation of these results to three dimensional structures with penetrations (deliberate or inadvertent) was beyond the scope of the effort; however, a baseline has been developed for the application of low level test procedures to EMP shielding effectiveness of shelters. Experimental verification was initiated on a screen room test bed. Unfortunately, the screen room was destroyed by fire prior to the completion of the tests and experimental verification of the theoretical results was not possible.

3.3 BACKGROUND

For nearly 20 years, MIL-STD-285 has been used by the Government as a standard for measuring the electromagnetic shielding characteristics of enclosures used to house electronic equipment. Procedures are defined for electric, magnetic, and plane wave testing which employ low-level signal generators or power oscillators to provide continuous wave (CW), modulated CW (MCW), or a pulsed CW signal. Power levels of transmitters and sensitivities of receivers/detectors must be compatible with measuring the shielding effectiveness of enclosures providing up to 100 dB of attenuation. In the case of electric and magnetic field measurements (dipole and loop), the transmitting and receiving antennas are located 12 inches (0.305 m) from the inner and outer surfaces of the shielded enclosure and measurements are taken at several frequencies. In addition to the loop and dipole procedures designed primarily for magnetic and electric field shielding effectiveness evaluation, the shield is also evaluated for plane wave performance. In this case, MIL-STD-285 calls for one test frequency, 400 MHz, and specifies that the transmitting antenna must be separated from the test object by at least six feet (1.83 m). The receiving antenna must be at least two inches (0.05 m) from the other side of the shield.

Because of the widespread familiarity in industry and DOD with MIL-STD-285 testing, and the availability of standard, acceptable test gear, it certainly is appealing to extrapolate these procedures to the EMP regime and it is not surprising that such has occurred - the same test procedures are now being specified in many cases by the DOD for EMP as have been used in the past for EMI, EMC, and TEMPEST.

It is not intuitively obvious that low-level CW shielding effectiveness test results taken in the near field are directly relatable to an electromagnetic pulse, a uniform plane wave with a short rise time and wide frequency content. A search of the literature reveals that analytical work has been done on this problem and that a theoretical solution has been offered. R. L. Monroe addressed EMP shielding effectiveness and MIL-STD-285 in Harry Diamond Laboratory TR-1636. This report concluded that measurements carried out in the manner prescribed by MIL-STD-285 using small CW dipole and loop sources located at fixed relative positions 12 inches (0.305 m) from the walls will give upper and lower bounds for the EMP shielding effectiveness of any metallic structure at all frequencies of interest from 10^2 to 10^9 Hz. Upper bounds are provided by dipole measurements and lower bounds by loop measurements for each frequency employed in MIL-STD-285 applicable to the frequency content of the pulse.

A closed form expressing $\delta(r, f)$ was developed in the report to provide the difference in shielding effectiveness offered by the shelter located in the far field and the shielding effectiveness offered by the same shelter located in the extreme near field of an antenna. This expression provided a correction factor to apply to MIL-STD-285 test readings to obtain the plane wave shielding effectiveness. The correction factor is a function of frequency (f) and distance (r) between the source and structure and depends upon the ratio between the wave impedances of the EMP, loop and dipole generated fields. The same correction factor is obtained for loop and dipole antennas located 12 inches (0.305 m) from the shelter wall. The correction factor is added to loop shielding effectiveness readings and subtracted from dipole readings.

Thus, within the constraints of the assumptions of the report, as discussed in Paragraph 3.4.3 below, the techniques of MIL-STD-285 are stated as being applicable to EMP shielding effectiveness testing.

3.4 EVALUATION OF HDL-TR-1636

3.4.1 Overview

HDL-TR-1636 took the first step in applying shielding effectiveness techniques developed over the years by the EMC community to the EMP problem. It attempted to apply low-level CW test procedures (MIL-STD-285) to EMP shielding effectiveness. The entire report has been reviewed for technical correctness and, within the stated assumptions, no errors of a technical nature were detected in the solution presented. As will be discussed below, however, we do take exception to the key assumption upon which the entire report rests. The author bases his discussion on the definition of shielding effectiveness as first presented by Schelkunoff, expands the effort in terms of transmission line theory and thereby assumes a plane electromagnetic wave incident on the shielding material. This assumption is at variance with the actual situation for MIL-STD-285 testing since the shield is in the extremely near field of antennas.

The other main reservation taken to the technical report lies in the references upon which the report is based. MIL-STD-285 requires that the loops employed over much of the range of frequencies of significance to EMP be oriented in a plane perpendicular to the wall under test - termed the coplanar orientation. All of the references quoted in the technical report address the situation where the loops are in planes parallel to each other and to the plane of the wall under test, the so-called "coaxial" orientation. No theoretical work has been discovered which addresses the MIL-STD-285 (copolanar) situation while many papers address the coaxial orientation. This

anomaly is further complicated by the fact that the wave impedance approach as introduced by Schelkunoff and employed by Monroe requires an orbitrary correction factor (a reduction by 1/3 in the distance between antennas) to obtain a correlation between theoretical and experimental results.

It was apparent at the completion of the initial investigation of HDL-TR-1636 that an independent assessment, free of any simplifying assumptions was advisable. The independent approach and the correlation of results between the two are in Paragraphs 3.5 and 3.6.

No attempt will be made here to present a complete review of the technical report. For that, the interested reader is referred to the original document.[1] Information will be presented that pertains to the concept of shielding effectiveness employed by the author and arguments presented to support the contention that an independent assessment is advisable.

At the time the review was accomplished and the exception taken, it was difficult to assess the relative magnitude of error caused by the simplifying assumptions. At the completion of the effort, we conclude that HDL-TR-1636 has considerable merit as an engineering approximation to the solution, especially in the lower frequency regime, a regime containing much of the energy content of the electromagnetic pulse.

Prior to proceeding, the abstract of HDL-TR-1636 is presented as an overview of the effort.

"The relationship between electromagnetic-pulse (EMP) shielding effectiveness and MIL-STD-285 is investigated analytically. It is found that measurements carried out in the manner prescribed by MIL-STD-285 using small cw dipole and loop sources located at fixed relative positions 12 in. from the walls will give upper and lower bounds for the EMP (plane wave) shielding effectiveness of any metallic structure at all frequencies of interest (10^{-2} to 10^{8} Hz). Upper bounds are provided by dipole measurements and lower bounds by loop measurements for each EMP frequency corresponding to a frequency employed in MIL-STD-285. A closed form expression δ (r, f) is obtained for the difference between EMP shielding effectiveness and loop shielding effectiveness. This expression is independent of any metallic structure and depends only on the ratio between wave impedances of the EMP and loop fields. That is, it depends only on the impedance mismatch between EMP and loop fields at the surface of the structure. In general, it is a function of frequency f and distance r between the source and structure. Since both EMP and loop wave impedances are known, δ (r, f) can be explicitly evaluated for a source distance of 12 in. and added to measured values of loop shielding effectiveness to give estimates of EMP shielding effectiveness at any frequency. A similar result is obtained for a dipole source. In this way, MIL-STD-285 measurements can be used to estimate EMP shielding effectiveness."

3.4.2 Shielding Effectiveness and Wave Impedance

The concept of shielding effectiveness, as first introduced by Schelkunoff[3] was defined in terms of transmission line theory and was applied to plane wave transmission through imperfectly conducting shields. Basically, Schelkunoff's original expression for shielding effectiveness is given by

$$S.E.\ (dB) = R + A + B$$

where R represents losses due to initial reflections, A is the loss due to attenuation of the field in penetrating the shield once, and B accounts for losses due to reflections which are not contained in R. This definition of shielding effectiveness is used quite universally by the EMC community.

MIL-STD-285, the shielding effectiveness measurement standard, states a conceptually simple definition of shielding effectiveness as

$$S.E.\ (dB) = 20 \log E_1/E_2$$

where E_1 is the electric field measured in the plane of the shield in the absence of the shield and E_2 is the field measured in the presence of the shield on the side of the shield away from the source. At the frequencies of interest in EMP fields, the shielding effectiveness of an enclosure is primarily determined by the ratio of reflected to incident signal energy. Thus, by far the most important term in Schelkunoff's shielding effectiveness equation is that due to reflections. As pointed out in HDL-TR-1636, the ratio of reflected to incident signal energy (indirectly E_1 and E_2 as required by the MIL-STD-285 definition above) depends critically on the ratio of wave impedances of the incident field to the impedance of the enclosure. The wave impedance of a source at a field point is a function of the type of source (loop, dipole, monopole, horn, etc.), distance and frequency. It is defined as the ratio of the electric field to the magnetic field in a plane transverse to the radius vector from the source to the field point and, in the case of a uniform plane wave (as assumed in the case of an EMP generated by a high altitude nuclear detonation) has the value of approximately 377 ohms.

To quote from HDL-TR-1636:

"The most important similarity between small loop and dipole sources and EMP sources lies in the fact that the wave impedances of all three sources are independent of spatial variations in directions transverse to the radius vector from the source to any field point. That is Z_{EMP}, Z_D, and Z_L (wave impedances for EMP, dipole and loop, respectively) are all independent of the transverse coordinates θ and ϕ. Z_{EMP} is a constant while Z_D and Z_L are functions of r alone. It was pointed out by Schelkunoff that if a field incident on an electrical discontinuity (such as an EMP shield) has an associated wave impedance which is independent of the transverse coordinates, and if the transmitted field also has an associated wave impedance which is independent of the transverse coordinates, then standard transmission line theory can be applied to compute the reflected and transmitted fields. This fact greatly simplifies the problem of estimating the shielding effectiveness seen by these three sources, and it ensures the existence of an analytical relation between SE_D, SE_L, and SE_{EMP}." (Shielding effectiveness to dipole, loop and EMP.)

Wave impedances may be calculated for the elementary dipole and loop source, antennas employed in the MIL-STD-285 technique, as indicated in Figure 3.4-1.

If an elementary dipole is located at the origin of a spherical coordinate system as indicated in Figure 3.4-1, the fields produced are[5]

$$H_{\phi} = \frac{I\ell \sin\theta}{4\pi r}\left(j\beta + \frac{1}{r}\right)e^{-j\beta r}$$

$$E_{\theta} = \frac{\eta I\ell \sin\theta}{4\pi r}\left(j\beta + \frac{1}{r} + \frac{1}{j\beta r^2}\right)e^{-j\beta r}$$

$$E_{r} = \frac{\eta I\ell \cos\theta}{2\pi r}\left(\frac{1}{r} + \frac{1}{j\beta r^2}\right)e^{-j\beta r}$$

where I is the source current, ℓ is the length of the short dipole, r, θ, and ϕ are spherical coordinates, and $\beta = 2\pi/\lambda$ where λ is the signal wavelength. Similarly, the fields generated by an elementary loop antenna are given by[6]

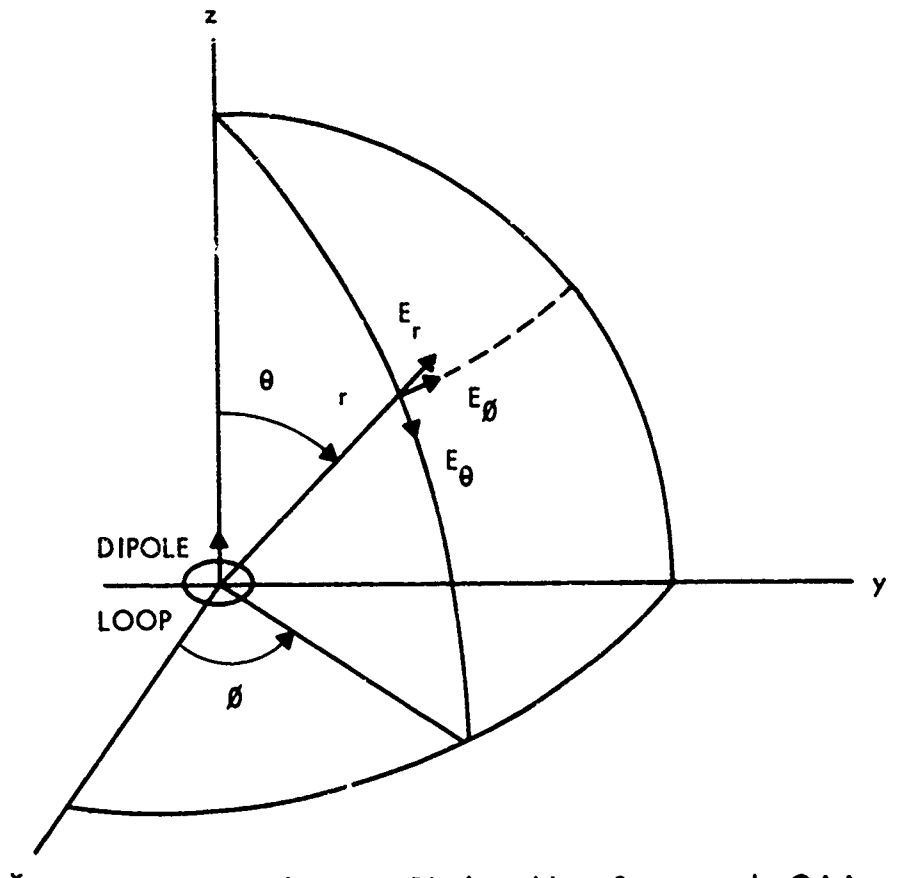

Figure 3.4-1. Elementary Dipole and Loop Sources at the Origin of a Spherical Coordinate System

$$E_{\phi} = \frac{\eta \beta^2 IA \sin\theta}{4\pi r} \left(1 + \frac{1}{j\beta r}\right) e^{-j\beta r}$$

$$H_{\theta} = -\frac{\beta^2 IA \sin\theta}{4\pi r} \left(1 + \frac{1}{j\beta r} - \frac{1}{\beta^2 r^2}\right) e^{-j\beta r}$$

$$H_{r} = \frac{j\beta IA \cos\theta}{2\pi r^2} \left(1 + \frac{1}{j\beta r}\right) e^{-j\beta r}$$

where A is the area of the loop source. These fields are valid provided the sources (with dimensions ℓ and A) are small compared to the radiated wavelength.

The main conclusion of HDL-TR-1636 is presented by the correction factor $\delta(r, f)$ which is given by the following equation and evaluated for c distance of 12 inches (0.035 m). The graphical result is reproduced in Figure 3.4-2 below:

$$\delta = -20 \log \left(\frac{|Z_{emp}|}{|Z_o|}\right) = 20 \log \left(\frac{|Z_{emp}|}{|Z_L|}\right)$$

where $Z_{emp} \cong 377\ \Omega$

$$Z_D = \frac{E_{\theta}}{H_{\phi}} = \eta \left(\frac{1 + j\beta r - \beta^2 r^2}{j\beta r - \beta^2 r^2}\right)$$

$$Z_L = \frac{E_{\phi}}{H_{\theta}} = \eta \left(\frac{j\beta r - \beta^2 r^2}{1 + j\beta r - \beta^2 r^2}\right)$$

The correction factor is symmetrical in that the same correction is added to loop readings as is subtracted from the dipole readings to obtain values of shielding effectiveness applicable to EMP.

3.4.3 Statement of Reservations

It was concluded at the time of the evaluation that this result should not be used in studies pertaining to EMP shielding effectiveness without the application of correction factors to account for the anomalies to be discussed below.

First, the basic equation by Schelkunoff assumes an incident plane wave in its derivation. In other words, Schelkunoff's transmission line theory cannot be applied when a spherical wave is incident upon a planar shield. Moser[4], one of the references in HDL-TR-1636 uses Schelkunoff's

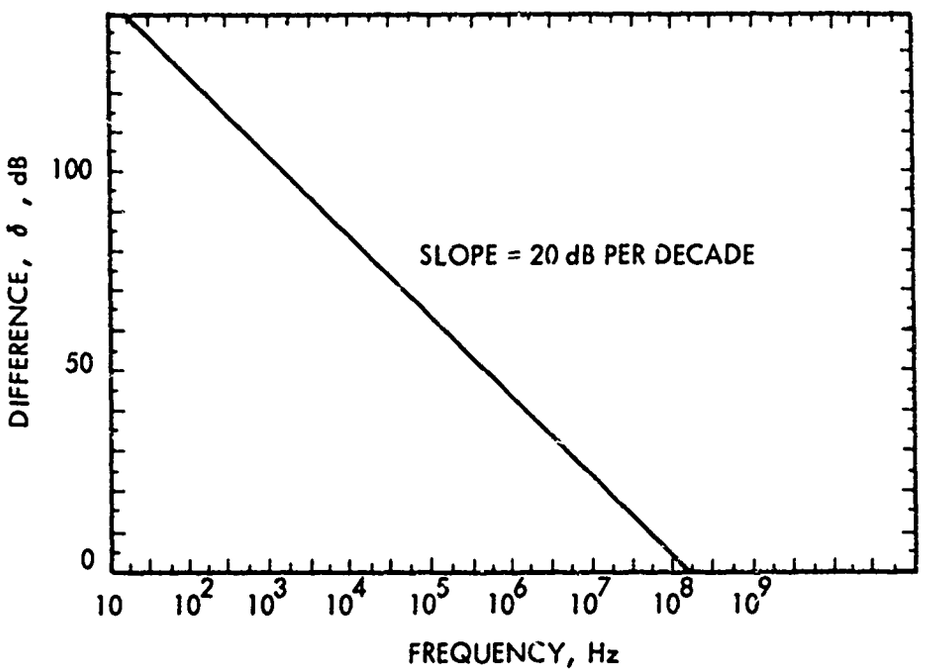

Figure 3.4-2. The Difference δ Between Shielding Effectiveness Measured with a Plane Wave Source and Shielding Effectiveness Measured with a Small Loop (or Dipole) Source Located at a Distance r = 12 Inches from the Shield

approach as one of his three techniques for computing the shielding effectiveness of a continuous planar shield to a small circular loop antenna. When using this equation, the disagreement between theoretical and measured results can be as much as 10 dB. This does not appear significant until one realizes that shelters are frequently rejected from vendors if tests show a deviation from specification by as little as 2 or 3 dB. Perhaps even more significant is the fact that the HDL report extends Schelkunoff's approach to compute shielding effectiveness for a perfectly conducting slotted shield - an extension which can lead to errors of larger and significant magnitude since wave impedance is not constant over the length of the slot. That is, if a source antenna is placed very close to a shield, the form of the incident waves will be of a complex spherical nature rather than planar. Thus, viewing the incident field to be comprised of an infinite number of transmitted rays, it is observed that each ray tranverses a different path length from the source to the shield. Consequently, at a given frequency, the wave impedance due to the source varies as one moves along at the surface of the shield. Therefore, the shielding effectiveness (as used in HDL-TR-1636) has a unique value at

each point on the surface of the continuous shield. If a fault is very small such that wave impedance is essentially constant over the region of the fault, then the magnitude of error is not significant. If, however, the fault is a crack, such as a door seam, the shielding effectiveness results will vary considerably.

Also, the equations of E and H fields for the elementary loop and dipole antennas are valid only if the source dimensions are small with respect to wavelength, perhaps one tenth of a wavelength. For the frequencies of conern in EMP analysis (10^2 to 10^8 Hz), these fields will not always be valid: this is especially true at the higher frequencies where the source dimensions are comparable to the wavelength. This does not invalidate the concept of wave impedance; it merely indicates that equations appropriate to this situation are required.

Finally, as indicated in the overview, all of the references quoted in the report relate to a loop antenna orientation at variance with MIL-STD-285 procedures and no analytical relationship has been discovered to correlate performance of these antennas as a function of orientation.

As indicated earlier, although exceptions may be taken to the approach, the results pertaining to the uniform plane shield are now considered a reasonable engineering approximation. Care must be exercised as one approaches frequencies where the test antennas constitute an appreciable portion of a wavelength. Also, the applicability of the work to faults in a shield is suspect because the wave impedance changes as a function of radial distance from the antenna.

3.5 PLANE WAVE SPECTRUM

In the paper by Booker and Clemmow[7] in April 1949, it was observed that the rectangular components of the electromagnetic field on one side of a planar aperture can be represented simply and exactly by a linear combination of plane waves. From this primitive mathmatical structure, representing the simplest possible boundary-value problem in electromagnetic radiation, some of the most interesting results in antenna theory were obtained. First, it was shown that the steady-state radiation pattern reduces to just an angular spectrum of these plane waves taken over all angles. Then it was shown that the pattern and aperture functions are obtainable from each other, and finally that those portions of the pattern function which correspond to complex angles determine completely the reactive energy stored about the aperture.

The concept of the plane wave spectrum is ideally suited to relating shielding effectiveness as measured by low-level CW sources in the near field to the shielding effectiveness presented by a shelter to a uniform plane wave. The following is the basic discussion of the method taken[8].

3.5.1 Plane Wave Expansion of Electromagnetic Waves

Let us consider the electromagnetic field ($\underline{E}$, $\underline{H}$) solution of the source free Maxwell's equations

$$\nabla \times \underline{E} = -j\omega\mu\underline{H} \qquad 3.5\text{-}1$$

$$\nabla \times \underline{H} = j\omega\epsilon\underline{E} \qquad 3.5\text{-}2$$

$$\nabla \cdot \underline{E} = 0 \qquad 3.5\text{-}3$$

$$\nabla \cdot \underline{H} = 0 \qquad 3.5\text{-}4$$

The environment is assumed homogeneous and isotropic, and steady-state conditions are postulated.

Assume now the spatial dependence of the fields to be of the type exp. ($-j\underline{K} \cdot \underline{r}$). Then, upon substitution into equation 3.5-1 through equation 3.5-4, the following result is obtained:

$$\underline{K} \times \underline{E} = \omega\mu\underline{H} \qquad 3.5\text{-}5$$

$$\underline{H} \times \underline{K} = \omega\epsilon\underline{E} \qquad 3.5\text{-}6$$

$$\underline{K} \cdot \underline{E} = 0 \qquad 3.5\text{-}7$$

$$\underline{K} \cdot \underline{H} = 0 \qquad 3.5\text{-}8$$

where $\underline{E}$ and $\underline{H}$ are spatially constant vectors, and $\underline{K}$ is the propagation vector.

Let us now cross multiply equation 3.5-5 by $\underline{K}$ from the right, and substitute from equation 3.5-6. We get

$$\underline{K} \times \underline{E} \times \underline{K} - \omega^2\epsilon\mu\underline{E} = 0 \qquad 3.5\text{-}9$$

However, equations 3.5-7 and 3.5-8 show that $\underline{E}$ and $\underline{H}$ are orthogonal. Then, letting $\omega^2\epsilon\mu = \beta^2$, where β is the free-space propagation constant

$$(K^2 - \beta^2)\underline{E} = 0 \qquad 3.5\text{-}10$$

Accordingly, the absolute value of $\underline{K}$ is determined, and equals β. Let K_x, K_y and K_z be the Cartesian components of $\underline{K}$,

$$\underline{K} = K_x \hat{x} + K_y \hat{y} + K_z \hat{z} . \qquad 3.5\text{-}11$$

It follows from $K = \beta$ that

$$K_z = \sqrt{\beta^2 - (K_x^2 + K_y^2)} \qquad 3.5\text{-}12$$

Accordingly, the (K_x, K_y) plane can be divided into two regions separated by a circle centered at the origin and of radius β. For the inner region, which is called the visible region, $K_x^2 + K_y^2 < \beta^2$ and K_z is real. The square root in equation 3.5-12 is taken with the positive sign, so that propogation along the positive direction of the z axis is assured. The propogation vector $\underline{K}$ is determined by direction cosines

$$\cos \phi_1 = \frac{K_x}{\beta} , \quad \cos \phi_2 = \frac{K_y}{\beta} , \quad \cos \theta = \frac{K_z}{\beta} \qquad 3.5\text{-}13$$

which correspond to real angles (see Figure 3.5-1).

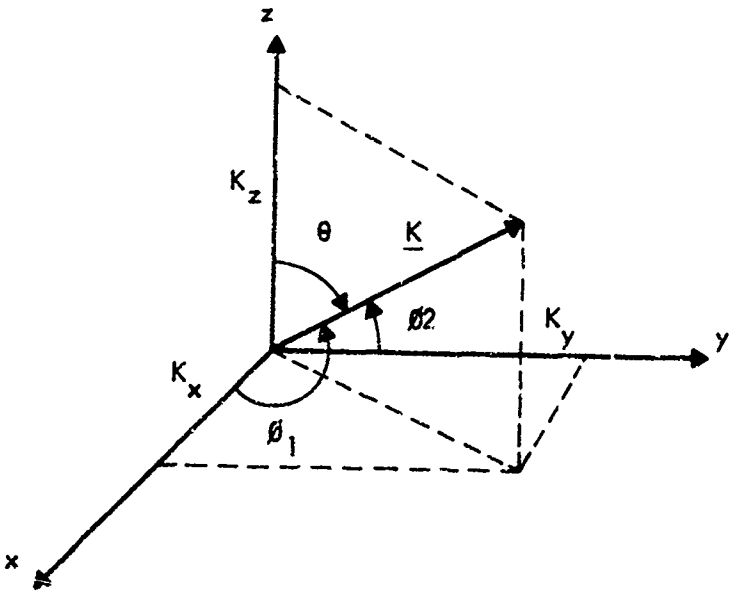

Figure 3.5-1. The K Vector

For $K_x^2 + K_y^2 = \beta^2$, $\theta = 90^\circ$ and the propagation vector $\underline{K}$ is parallel to the $z = 0$ plane.

For $K_x^2 + K_y^2 > \beta^2$, which defines the invisible region, K_z is pure imaginary and we take

$$K_z = -i\,|K_z| = -i\sqrt{\left(K_x^2 + K_y^2\right) - \beta^2} \qquad 3.5\text{-}14$$

where

$$K_x^2 + K_y^2 > \beta^2$$

so that damping of the wave along the positive direction of the z axis is assured.

Real values of K_z correspond to the usual plane waves, while imaginary values correspond to surface waves linked to the plane $z = 0$ and exponentially attenuated for $z > 0$.

Just as $\underline{K}$ components are not all independent, $\underline{E}$ and $\underline{H}$ components are also mutually related. In particular

$$Z_{air}\,\underline{H} = \frac{\underline{K} \times \underline{E}}{\beta} \qquad 3.5\text{-}15$$

from equation 3.5-5,

where $Z_{air} = \sqrt{\frac{\mu}{\epsilon}}$, and

$$E_z = -\frac{K_x E_x + K_y E_y}{K_z} \qquad 3.5\text{-}16$$

from equation 3.5-7.

Under rather general conditions, an electromagnetic field $(\underline{E}, \underline{H})$ can be expanded in a set of plane waves. Hence, for $z > 0$

$$\underline{E}(x, y, z) = \int_{-\infty}^{\infty}\int_{-\infty}^{\infty} \underline{\mathcal{E}}(K_x, K_y)\, e^{-i\left(K_x x + K_y y + K_z z\right)} dK_x\, dK_y \qquad 3.5\text{-}17$$

where

$$\underline{\mathcal{E}}\,(K_x, K_y) = \text{the plane wave spectrum.}$$

Note that $\underline{\mathcal{E}}$, which is (K_x, K_y) dependent, is a density of electric field per square wave number. Obviously, the formal superposition of equation 3.5-17 is of practical use if the vector function $\underline{\mathcal{E}}$ can be determined once the sources of $\underline{E}$ are given.

3.5.2 Radiation from an Aperture-Spectrum Calculation

If we now cross-multiply equation 3.5-17 by $\hat{z}$ from both the left and the right and specify the result for $z = 0$, i.e., in the x - y plane aperture, we get

$$\hat{z} \times \underline{E}\,(x, y, 0) \times \hat{z} = \int_{-\infty}^{\infty}\int_{-\infty}^{\infty} \hat{z} \times \underline{\mathcal{E}}\,(K_x, K_y) \times \hat{z}\; e^{-j\left(K_x x + K_y y\right)} dK_x\, dK_y \qquad 3.5\text{-}18$$

Note that $\hat{z} \times \underline{E}\,(x, y, 0) \times \hat{z} = \underline{E}_t^a\,(x, y)$ is the tangential component of the electric field in the plane $z = 0$, i.e., the applied electric field across the aperture. Letting $\hat{z} \times \underline{\mathcal{E}}\,(K_x, K_y) \times \hat{z} = \underline{\mathcal{E}}_t\,(K_x, K_y)$, equation 3.5-18 can be rewritten as

$$\underline{E}_t^a\,(x, y) = \int_{-\infty}^{\infty}\int_{-\infty}^{\infty} \underline{\mathcal{E}}_t(K_x, K_y)\, e^{-j\left(K_x x + K_y y\right)}\, dK_x\, dK_y \quad . \qquad 3.5\text{-}19$$

Equation 3.5-19 shows the tangential electric field across the aperture to be the double Fourier transform of the tangential components of the plane wave expansion of the electric field associated with the aperture.

It is thus possible to show the conclusion of Booker and Clemmou that the angular plane wave spectrum is the inverse double Fourier transform of the aperture distribution as:

$$\underline{\mathcal{E}}_t\,(K_x, K_y) = \frac{1}{(2\pi)^2} \iint \underline{E}_t^a\,(x, y)\, e^{\,j\left(K_x x + K_y y\right)}\, dx\, dy \qquad 3.5\text{-}20$$

The vector $\underline{\mathcal{E}}_t\,(K_x, K_y)$ is called the "spectrum" or "spatial spectral components", associated with the aperture: in an analogous manner, $\underline{K}$ is called the "spatial frequency" associated with the aperture. The third component of the complete plane-wave expansion can be obtained via equation 3.5-16.

3.5.3 Complex Power Spectrum Calculation

Only a limited region of the Plane Wave Spectrum can be identified with the radiation pattern, namely, those values of K_x and K_y corresponding to real values of K_z. The rest is invisible. To repeat from the development above, if K_x and K_y are varied in equation 3.5-12 beyond a certain circular region in the $K_x - K_y$ plane given by $K_x^2 + K_y^2 = \beta^2$, K_z becomes imaginary. The region outside this circle is defined as the invisible region. The circular visible region corresponds to the real radiation pattern while the invisible region accounts for reactive energy stored in the field about the aperture and corresponds to surface waves which are linked to the plane $z = 0$ and which are exponentially attenuated for $z > 0$. Since this reactive energy is relatively large compared to the real energy in the near field, the reactive coupling is of fundamental importance in the problems associated with the shielding effectiveness as measured by low level CW sources in the near field.

The mean power flow across the aperture plane is represented by the normal component of the complex Poynting vector integrated over the plane $z = 0$, which vanishes outside of the aperture S:

$$-1/2\int_S \underline{E} \times \underline{H}^* \cdot \hat{z}\, da = 1/2\iint_S \left(\frac{K^* |E^{TE}|^2}{\zeta Z_{air}} - \frac{K Z_{air} |H^{TM}|^2}{\beta}\right) \cdot \hat{z}\, dx\, dy \qquad 3.5\text{-}21$$

The first term on the right is the sole contributor to the power produced by the TE partial field, and the second to the power produced by the TM partial field.

By applying Parseval's theorem, equation 3.5-21 can be transformed as follows:

$$-\frac{(2\pi)^2}{2}\int_{-\infty}^{\infty}\int_{-\infty}^{\infty} \underline{\mathcal{E}} \times \underline{\mathcal{H}}^* \cdot \hat{z}\, dK_x\, dK_y = \frac{(2\pi)^2}{2}\int_{-\infty}^{\infty}\int_{-\infty}^{\infty}\left(\frac{K_z^*}{\beta}\frac{|\mathcal{E}^{TE}|^2}{Z_{air}} - \frac{K_z}{\beta} Z_{air} |\mathcal{H}^{TM}|^2\right) dK_x\, dK_y \qquad 3.5\text{-}22$$

where $\underline{\mathcal{E}}$ and $\underline{\mathcal{H}}$ are the electric and magnetic field components of the plane wave spectrum and and $\mathcal{E}^{TE}$ is the electric field plane wave spectrum of the TE partial field and $\mathcal{H}^{TM}$ is the magnetic field plane wave spectrum of the TM partial field.

From the left-hand side, the real part represents real power leaving the aperture to be radiated away, while its imaginary part represents reactive power (2π times the difference between the mean values of the magnetic and the electric energies stored on the + z side of the aperture). On the right-hand side it is seen that the only complex quantity involved is K_z and its complex conjugate. They are both purely real when $K_x^2 + K_y^2 < \beta^2$ and purely imaginary when $K_x^2 + K_y^2 > \beta^2$. Consequently, the visible region of radiated power is the interior of the circle $K_x^2 + K_y^2 = \beta^2$ and the invisible region of reactive power is all the rest of the (K_x, K_y) plane.

3.6 APPLICATION OF THE PLANE WAVE SPECTRUM TO SHIELDING EFFECTIVENESS

3.6.1 Introduction

Based upon the plane wave spectrum concept presented above, it is now desirable to provide the necessary mathematical rigor to show the applicability of the concept to the shielding effectiveness problem utilizing small loops and dipoles in the near field.

Maxwell's source free equations in free space can be expressed in two separate sets of equations representing TM and TE waves. In spherical coordinates the TM waves are given by

$$-j\omega\mu H_\phi = \frac{1}{r}\frac{\partial}{\partial r}\left(r E_\theta\right) - \frac{1}{r}\frac{\partial}{\partial \theta} E_r$$

$$j\omega\epsilon E_r = \frac{1}{r\sin\theta}\frac{\partial}{\partial \theta}\left(\sin\theta\ H_\phi\right)$$

$$j\omega\epsilon E_\theta = \frac{1}{r}\frac{\partial}{\partial r}\left(r H_\phi\right)$$

which are used to develop the fields associated with a small dipole. Similarly, TE waves are given by

$$j\omega\epsilon E_\phi = \frac{1}{r}\frac{\partial}{\partial r}\left(r H_\theta\right) - \frac{1}{r}\frac{\partial}{\partial \theta} H_r$$

$$-j\omega\mu H_r = \frac{1}{r\sin\theta}\left(\frac{\partial}{\partial \theta}\sin\theta\ E_\phi\right)$$

$$-j\omega\mu H_\theta = \frac{1}{r}\frac{\partial}{\partial r}\left(r E_\theta\right)$$

which are used to develop the fields associated with small loops.

The plane wave expansion material of Paragraph 3.5 yields a set of TM and TE waves for a given propagation vector $\underline{K}$ and, in the plane wave concept, only the fundamental set (TM for dipole and TE for loop) should be used for the respective radiators. In effect, the plane wave spectrum yields a general solution composed of a linear combination of TE and TM waves for a given antenna in the near field. Since the elementary dipole does not radiate TE waves in the near field, the TM waves must be extracted from the solution and used in subsequent calculations. Similar reasoning applies for the loop antenna. This concept governs all subsequent treatment of the problem and the remaining discussions will be structured accordingly. Also, the approach concentrates initially on a representative member of the family of plane waves. After the relationships for power flow have been developed, we will again return to the concept of the family of plane waves.

3.6.2 Incident Power for Loop Antennas - TE Expansion

With reference to the coordinate system shown in Figure 3.6-1 we can represent the $\underline{E}$ field associated with a plane wave as

$$\underline{E} = E_0 \, e^{-i \underline{K} \cdot \underline{r}}$$

where $\underline{K} = K_x \hat{x} + K_y \hat{y} + K_z \hat{z}$ is, as before, the propagation vector. It should be noted that the aperture in the x-y plane of Figure 3.6-1 is also the plane of the shielding structure being investigated.

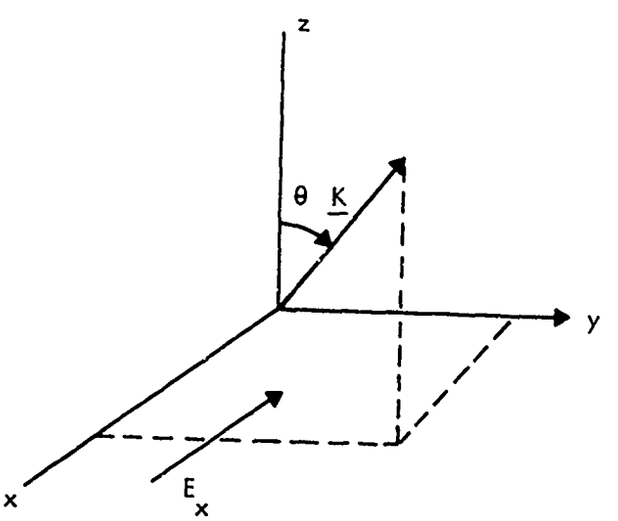

Figure 3.6-1. Coordinate System for TE Expansion

We can determine the magnitude of the $\underline{K}$ components by the dispersion relation where

$$K_0^2 = K_x^2 + K_y^2 + K_z^2 = \omega^2 \mu \epsilon .$$

You will recall from the development of Paragraph 3.5 that K_0^2 equals the free space propagation constant squared, β^2. As long as $K_x^2 + K_y^2$ remains smaller than K_0^2 we will remain in the visible region. If however $K_x^2 + K_y^2$ exceeds K_0^2 we move into the invisible region or $K_z = -j\,|K_z|$.

In the visible region,

$$j\underline{K} = j\left(K_x\,\hat{x} + K_y\,\hat{y} + K_z\,\hat{z}\right) = j\beta$$

and for the invisible region,

$$j\underline{K} = j\left(K_x\,\hat{x} + K_y\,\hat{y}\right) + |K_z|\,\hat{z} = \alpha + j\beta$$

In order to obtain the transverse electric field it is necessary to define a unit vector that is perpendicular to $\underline{K}$ for both the visible and invisible regions. In other words, for a given propagation direction (K_x, K_y specified), the component of the electric field perpendicular to the plane of propagation must be determined in order to extract the TE waves from the general spectral solution. This may be accomplished by the following mathematic manipulation.

$$\frac{\underline{\alpha} \times \underline{\beta}}{|\underline{\alpha} \times \underline{\beta}|} = \frac{-K_y |K_z|\,\hat{x} + K_x |K_z|\,\hat{y}}{\sqrt{K_y^2 |K_z|^2 + K_x^2 |K_z|^2}} \quad \text{or}$$

$$\frac{\underline{\alpha} \times \underline{\beta}}{|\underline{\alpha} \times \underline{\beta}|} = \frac{-K_y\,\hat{x} + K_x\,\hat{y}}{\sqrt{K_y^2 + K_x^2}} = \widehat{\underline{\alpha} \times \underline{\beta}}$$

This is the unit vector perpendicular to the $\underline{K}$ vector.

If the electric field is given by

$\underline{E} = E_x\,\hat{x} + E_z\,\hat{z}$ (linearly polarized in the x direction)

the transversal projection of $\underline{E}$ is

$$\underline{E} \cdot \widehat{\underline{\alpha} \times \underline{\beta}} = \frac{-E_x K_y}{\sqrt{K_y^2 + K_x^2}} = E \widehat{\underline{\alpha} \times \underline{\beta}}$$

The transversal electric field vector is thus

$$E \widehat{\underline{\alpha} \times \underline{\beta}} \quad \widehat{\underline{\alpha} \times \underline{\beta}} = \frac{E_x \left(K_y^2 \hat{x} - K_x K_y \hat{y} \right)}{K_y^2 + K_x^2} = \underline{E}_{TE}$$

We can also find the square of magnitude of this vector as:

$$\left| E_{TE} \right|^2 = \left| E_x^2 \right| \frac{K_y^2}{K_y^2 + K_x^2} \qquad 3.6\text{-}1$$

This expression will be required in the calculation of power below.

3.6.3 Incident Loop Power in the Visible Range

In order to obtain the incident power in the z direction (aperture in the x - y plane), we first derive the Poynting vector for the TE waves, and then obtain the component in the z direction by taking the scalar product with $\hat{z}$.

$$S_{TE} = \left(\frac{-\underline{K}^*}{2 \omega \mu} \underline{E}_{TE} \cdot \underline{E}^*_{TE} \right) \cdot \hat{z} \quad .$$

Recalling that $Z_{air} = \sqrt{\frac{\mu}{\epsilon}}$ and $K_0 = \omega \sqrt{\mu \epsilon}$ we may express $\omega \mu$ as $K_0 Z_{air}$ and S_{TE} as

$$S_{TE} = \frac{K_z}{2 K_0 Z_{air}} \left| E_{TE} \right|^2 \quad .$$

Substituting equation 3.6-1 for $|E_{TE}|^2$ results in

$$S_{TE} = \frac{1}{2 Z_{air}} \frac{K_z}{K_0} |E_x|^2 \quad \frac{K_y^2}{K_y^2 + K_x^2} \quad , \text{ the Poynting vector for a}$$

representative member of the TE family of plane waves. To compute the incident loop power, we now integrate over the spectrum, $(\mathcal{E}_x)$, in the wave number domain, applying Parseval's theorem as in equation 3.5-22 above.

$$P_{TE} = \frac{2\pi^2}{Z_{air}} \iint_{\substack{\text{visible} \\ \text{region}}} \frac{K_z}{K_0} |\mathcal{E}_x|^2 \frac{K_y^2}{K_y^2 + K_x^2} \, dK_x \, dK_y \qquad 3.6.2$$

where P_{TE} is the incident power.

3.6.4 Incident Loop Power in the Invisible Region

In a similar fashion we can obtain the incident power in the invisible region - the difference being in the definition of $\underline{K}$. With reference to equation 3.5-14, the vector $\underline{K}$ becomes

$$\underline{K} = K_x \hat{x} + K_y \hat{y} - i |K_z| \hat{z} \text{ and } -K^* \cdot \hat{z} = i |K_z| .$$

Therefore the power in the invisible range is given by

$$P_{TE} = \frac{i\, 2\pi^2}{Z_{air}} \iint_{\substack{\text{invisible} \\ \text{region}}} \frac{|K_z|}{K_0} |\mathcal{E}_x|^2 \frac{K_y^2}{K_y^2 + K_x^2} \, dK_x \, dK_y$$

3.6.5 Transmission Coefficients for TE Waves

Shielding effectiveness is basically the ratio of the incident power to the transmitted power. We have already derived an equation for the incident power and now must transport this power through the shield using the appropriate mechanism. From reference 9 the transmission coefficient for a TE wave is given by

$$T_{TE} = \frac{2}{1 + (\mu K_{Tz} / \mu_T K_z)}$$

where K_z is the z component of $\underline{K}$ and K_{Tz} is the z component of $\underline{K}_T$. The coordinate system and symbology used for this development are as indicated in figure 3.6-2.

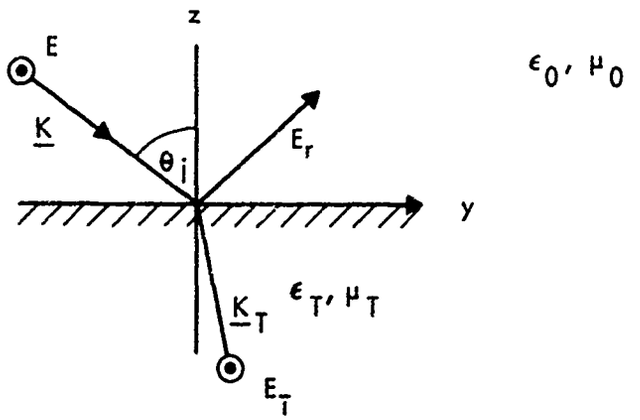

Figure 3.6-2. Geometry in the Plane of Incidence for TE Waves

In this coordinate system the transmitted Poynting vector in the -z direction is given by

$$S_{TE} = \frac{K_{Tz}}{\omega \mu_T} \left| T_{TE} \right|^2 \left| E_{TE} \right|^2 .$$

All of the factors of this equation are known except K_{Tz} which may be obtained as follows.

In metal, K_T is given by

$$K_T = \omega \left[\mu_T \left(\epsilon_0 + i \frac{\sigma}{\omega} \right) \right]^{1/2} .$$

However, in a good conductor such as aluminum or copper, σ is of the order of 10^7. Since the frequency range of interest is 10^2 to 10^8 Hz, ϵ_0 remains very small relative to the factor $\frac{\sigma}{\omega}$ and can be neglected. Thus, K_T may be expressed as

$$K_T = \left[i \omega \mu_T \sigma \right]^{1/2}$$

and

$$K_T^2 = i \omega \mu_T \sigma .$$

By applying the concept of phase matching[9] along the interface we find that $K_z = K_{Tz}$ therefore we obtain the following expression for K_{Tz} .

$$K_{Tz} = \sqrt{K_T^2 - K_y^2} \qquad 3.6\text{-}3$$

Equation 3.6-3 can also be expressed as:

$$\frac{K_{Tz}}{K_T} = \sqrt{1 - \frac{K_y^2}{K_T^2}}$$

Substituting $K_T^2 = j\,\omega\,\mu_T\,\sigma$ we obtain

$$K_{Tz} = K_T \sqrt{1 - \frac{K_y^2}{j\,\omega\,\mu_T\,\sigma}} = K_T \sqrt{1 + \frac{jK_y^2}{\omega\,\mu_T\,\sigma}} \quad .$$

Removing the imaginary component leaves

$$K_{Tz} = K_T \sqrt{1 + \frac{K_y^2}{\omega\,\mu_T\,\sigma}} \exp \frac{j \tan^{-1} \dfrac{K_y^2}{\omega\,\mu_T\,\sigma}}{2}$$

For a good conductor $\dfrac{K_y^2}{\omega\,\mu_T\,\sigma}$ is quite small and $K_{Tz} \approx K_T$.

Upon reflection, it is possible at this point to simplify the expression for the transmission cooefficients as well as the Poynting vector and express them in terms of parameters associated with the impedance of the shield and the propogation vector. We proceed in the following manner:

Starting with the same expression for the transmission coefficient for a TE wave[9], as

$$T_{TE} = \frac{2}{1 + \left(\mu K_{Tz} / \mu_T K_z\right)} = \frac{2}{1 + \left(\dfrac{K_{Tz}}{\mu_T} \Big/ \dfrac{K_z}{\mu}\right)}$$

we must manipulate our known equations to obtain new expressions for K_{Tz}/μ_T and K_z/μ. For purposes of illustration they will be obtained as follows:

First,
$$K_{Tz} = K_T \left(\frac{K_{Tz}}{K_T} \right)$$

and

$$K_{Tz} Z_s = \omega \sqrt{\mu_T \epsilon_T} \sqrt{\frac{\mu_T}{\epsilon_T}} \left(\frac{K_{Tz}}{K_T} \right)$$

$$= \omega \mu_T \left(\frac{K_{Tz}}{K_T} \right)$$

where Z_s is the impedance of the shield. Therefore,

$$\frac{K_{Tz}}{\mu_T} = \frac{\omega}{Z_s} \left(\frac{K_{Tz}}{K_T} \right)$$

Similarly, $\frac{K_z}{\mu} = \frac{\omega}{Z_{air}} \left(\frac{K_z}{K_0} \right)$.

Substituting these expressions into the transmission coefficient equation produces

$$T_{TE} = \frac{2 Z_s \left(\frac{K_z}{K_0} \right)}{Z_s \left(\frac{K_z}{K_0} \right) + Z_{air} \left(\frac{K_{Tz}}{K_T} \right)} \approx \frac{2 Z_s}{Z_{air}} \left(\frac{K_z}{K_0} \right) .$$

Therefore for both the visible and invisible regions

$$\left| T_{TE} \right|^2 = \frac{4 \left| Z_s \right|^2}{\left(Z_{air} \right)^2} \frac{\left| K_z \right|^2}{K_0^2} .$$

The Poynting vector becomes

$$S_{TE} = \frac{\omega\left(\frac{K_{Tz}}{K_z}\right)}{\omega Z_s} \cdot \frac{4\left|Z_s\right|^2}{\left(Z_{air}\right)^2} \frac{\left|K_z\right|^2}{K_0^2} \left| E_{TE} \right|^2$$

We can now obtain the power transmitted by the TE waves as

$$P_{TE} = (2\pi)^2 \frac{2\left|Z_s\right|}{\left(Z_{air}\right)^2} \iint_{\text{all regions}} \frac{\left|K_z\right|^2}{K_0^2} \left|\mathcal{E}_x\right|^2 \frac{K_y^2}{K_y^2 + K_x^2} \, dK_x \, dK_y$$

As before, we integrate over the spectrum, $(\mathcal{E}_x)$ in the wave number domain and apply Parseval's theorem.

3.6.6 Incident Power for the Dipole Antenna - TM Expansion

As in the TE expressions the first step is to calculate the transversal field vector. Here, however, it is the magnetic transversal field vector and is obtained using $\underline{H}$ fields. Let us start with $\underline{H}_0$ as

$$\underline{H}_0 = \frac{j\,\underline{K} \times \underline{E}}{j\,K_0 Z_{air}} = \frac{\underline{K} \times \underline{E}}{K_0 Z_{air}} \quad \text{or}$$

$$\underline{H}_0 = \frac{1}{K_0 Z_{air}} \left(K_x \hat{x} + K_y \hat{y} + K_z \hat{z}\right) \times \left(E_x \hat{x} + E_z \hat{z}\right).$$

Performing the indicated manipulation we have

$$\underline{H}_0 = \frac{1}{K_0 Z_{air}} \left(K_y E_z \hat{x} + \left(K_z E_x - K_x E_z \right) \hat{y} - K_y E_x \hat{z} \right)$$

Likewise the unit vector perpendicular to the $\underline{K}$ vector is

$$\widehat{\underline{\alpha} \times \underline{\beta}} = \frac{-K_y \hat{x} + K_x \hat{y}}{\sqrt{K_y^2 + K_x^2}}$$

We obtain the projection of $\underline{H}_0$ onto $\widehat{\underline{\alpha} \times \underline{\beta}}$ by taking the dot product, and, using the same terminology, obtain:

$$H_{\widehat{\underline{\alpha} \times \underline{\beta}}} = \frac{1}{K_0 Z_{air}} \left(-K_y^2 E_z + K_x \left(K_z E_x - K_x E_z \right) \right) \frac{1}{\sqrt{K_y^2 + K_x^2}} .$$

The transversal magnetic field vector is then

$$H_{\widehat{\underline{\alpha} \times \underline{\beta}}} \widehat{\underline{\alpha} \times \underline{\beta}} = \frac{\left(-K_y^2 E_z + K_x K_z E_x - K_x^2 E_z \right) \left(-K_y \hat{x} + K_x \hat{y} \right)}{K_0 Z_{air} \left(K_y^2 + K_x^2 \right)}$$

which yields

$$\underline{H}_{TM} = \left(\frac{K_x}{K_z} \right) \frac{E_x K_0}{Z_{air} \left(K_y^2 + K_x^2 \right)} \left(-K_y \hat{x} + K_x \hat{y} \right)$$

and

$$\left| H_{TM} \right|^2 = \frac{K_x^2}{\left| K_z \right|^2} \quad \frac{\left| E_x \right|^2 K_0^2}{\left(K_y^2 + K_x^2 \right) Z_{air}^2} \quad .$$

As before, this expression will be required in the power calculation.

3.6.7 Incident Power for the Dipole in the Visible Range

The Poynting vector for the dipole in the Z direction is given by

$$S_{TM} = \left(1/2 \quad \frac{\underline{K} \left(\underline{H} \cdot \underline{H}^* \right)}{\omega \epsilon} \right) \cdot \hat{z}$$

Since $\frac{K_0}{Z_{air}} = \omega \sqrt{\epsilon \mu} \sqrt{\frac{\epsilon}{\mu}} = \omega \epsilon$,

we can write the Poynting vector as

$$S_{TM} = \left(1/2 \quad \frac{Z_{air}}{K_0} \underline{K} \left(\underline{H} \cdot \underline{H}^* \right) \right) \cdot \hat{z} \quad .$$

In the visible range

$$\underline{K} = \left(K_x \hat{x} + K_y \hat{y} + K_z \hat{z} \right)$$

therefore S_{TM} reduces to

$$1/2 \quad \frac{Z_{air} K_z}{K_0} \quad \left(\underline{H} \cdot \underline{H}^* \right) \quad .$$

We can replace $\left(\underline{H} \cdot \underline{H}^*\right)$ by $\left| H_{TM} \right|^2$ and arrive at

$$S_{TM} = 1/2 \frac{K_0}{Z_{air}} \frac{\left| E_x \right|^2}{K_z} \frac{K_x^2}{\left(K_y^2 + K_x^2\right)} .$$

The incident power for the visible range thus becomes

$$P_{TM} = \frac{(2\pi)^2}{2 Z_{air}} \iint_{\text{visible range}} \frac{K_0}{K_z} \left| \mathcal{E}_x \right|^2 \frac{K_x^2}{K_y^2 + K_x^2} \, dK_x \, dK_y$$

3.6.8 Incident Power for the Dipole in the Invisible Region

Incident power in the invisible region is derived in a similar fashion except that $\underline{K} \cdot \hat{z} = -j \left| K_z \right|$ compared to $\overline{K} \cdot \hat{z} = K_z$ in the visible range. This difference results in the incident power being

$$P_{TM} = \frac{-j(2\pi)^2}{2 Z_{air}} \iint_{\text{invisible range}} \frac{K_0}{\left| K_z \right|} \left| \mathcal{E}_x \right|^2 \frac{K_x^2}{K_y^2 + K_x^2} \, dK_x \, dK_y$$

3.6.9 Transmission Coefficients for TM Waves

From reference 9 the transmission coefficient is given by:

$$T_{TM} = \frac{2}{1 + \left(\epsilon K_{Tz} / \epsilon_T K_z \right)}$$ where the same symbology is used. The transmitted Poynting vector in the -z direction is given by

$$S_{TM} = Z_s \left(\frac{K_{Tz}}{K_T} \right) \left| T_{TM} \right|^2 \left| H_{TM} \right|^2 .$$

If expressions are derived for $\frac{K_z}{\epsilon}$ and $\frac{K_{Tz}}{\epsilon_T}$ as derived before for $\frac{K_z}{\mu}$ and $\frac{K_{Tz}}{\mu_T}$ we obtain

$$\frac{K_z}{\epsilon} = Z_{air}\,\omega \quad \frac{K_z}{K_0}$$

and

$$\frac{K_{Tz}}{\epsilon_T} = \omega Z_s \left|\frac{K_{Tz}}{K_T}\right| \quad .$$

Substituting these expressions into T_{TM} we obtain

$$T_{TM} = \frac{2 Z_{air}\left(\frac{K_z}{K_0}\right)}{Z_{air}\left(\frac{K_z}{K_0}\right) + Z_s} \quad .$$

Since Z_s is very small in relation to $Z_{air}\left(\frac{K_z}{K_0}\right)$ the expression reduces to $T_{TM} \approx 2$. In turn, S_{TM} becomes

$$S_{TM} = \frac{4\left|Z_s\right|}{\left(Z_{air}\right)^2}\left(\frac{K_0^2}{\left|K_z\right|^2}\right)\left|E_x\right|^2 \quad \frac{K_x^2}{K_y^2 + K_x^2} \quad .$$

Integrating as before we obtain the transmitted power for all regions as

$$P_{TM} = (2\pi)^2 \quad \frac{2\left|Z_s\right|}{\left(Z_{air}\right)^2} \iint_{\substack{\text{All} \\ \text{regions}}} \frac{K_0^2}{\left|K_z\right|^2} \quad \left|\mathcal{E}_x\right|^2 \quad \frac{K_x^2}{K_y^2 + K_x^2}\, dK_x\, dK_y \quad .$$

3.6.10 Computation of Shielding Effectiveness Using the Plane Wave Spectrum

Prior to presenting the results of the Plane Wave Spectrum approach to shielding effectiveness and comparing those results with the results of HDL-TR-1636, it is appropriate to show that the definition of shielding effectiveness used in this report is compatible with the Schelkunoff approach as employed in HDL-TR-1636[1]. Also, an expression is presented which shows why the Plane Wave Spectrum technique provides more accurate results.

As developed by Schelkunoff and employed in HDL-TR-1636, shielding effectiveness is defined as:[11]

$$SE = R + A + B$$

where $$R = 20 \log \left[\frac{|K+1|^2}{4|K|} \right] ,$$

$$K = \frac{Z_{wave}}{Z_{shield}} \quad \text{(Impedance Ratio of source and shield)}$$

$$A = (8.686)\,\gamma t$$

$$\gamma = (\pi \mu \sigma f)^{1/2} \quad \text{(Reciprocal of skin depth)}$$

t = thickness of shield.

Since the penetration loss (A) is greater than 10 dB, reflections inside the shield may be neglected.[11]

Thus,

$$SE\ (dB) = 20 \log \left[\frac{\left| \frac{Z_w}{Z_s} + 1 \right|^2}{2\sqrt{\left| \frac{Z_w}{Z_s} \right|}} \right]^2 + 8.686\,\gamma t$$

Under the assumption that $\frac{Z_{wave}}{Z_{shield}} \gg 1$, this expression reduces to

$$SE\ (dB) = 20 \log \frac{Z_{wave}}{4Z_{shield}} + 8.686\ \gamma t$$

The definition of shielding effectiveness as used in this report was derived to facilitate the use of the Plane Wave Spectrum technique as

$$SE = 2\left(10 \log \left|\frac{P_{inc}}{P_{tr}}\right|\right) + 8.686\,\gamma t = R + A$$

In this case, the factor R is defined as the ratio of the power incident on the shield to the power transmitted at the plane of the shield as shown in Figure 3.6-3. The power transmitted, P_{tr}, is a function of the impedance mismatch at the incident plane of the shield. This mismatch exists at both sides of the shield thus the factor of two (2) is introduced in the term for R above.

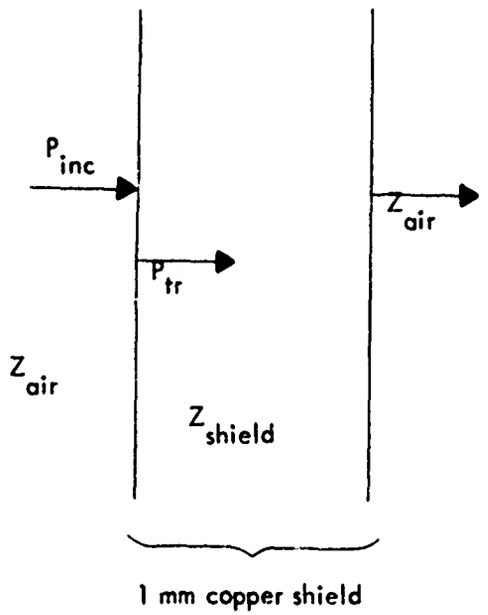

Figure 3.6-3. Shielding Effectiveness

We will now show that this definition of shielding effectiveness is compatible with that employed in HDL-TR-1636. For the case of the loop,

$$P_{TE}(Inc) = \frac{2\pi^2}{Z_{air}} \iint_{visible} \left|\frac{K_z}{K_o}\right| \left|\mathcal{E}_x^2\right| \frac{K_y^2}{K_y^2 + K_x^2}\, dK_x\, dK_y$$

over the visible region and

$$P_{TE}(Inc) = j\,\frac{2\pi^2}{Z_{air}} \iint_{invisible} \left|\frac{K_z}{K_o}\right| \left|\mathcal{E}_x^2\right| \frac{K_y^2}{K_x^2 + K_y^2}\, dK_x\, dK_y$$

over the invisible region. Also,

$$P_{TE}\ (\text{trans}) = \frac{(2\pi)^2 (2)\ |Z_s|}{(Z_{air})^2} \iint_{\text{all regions}} \frac{|K_z|^2}{K_o^2} |\mathcal{E}_x|^2 \frac{K_y^2}{K_x^2 + K_y^2}\ d K_x\, d K_y$$

For a plane wave traveling in the position Z direction in the visible region,

$K_x = K_y = 0$ and

$K_z = K_o$ thus,

$$\frac{P_{TE}\ (\text{Inc})}{P_{TE}\ (\text{trans})} = \frac{\frac{2\pi^2}{Z_{air}}}{\frac{(2\pi)^2\ (2)\ (Z_s)}{Z_{air}^2}} = \frac{Z_{air}}{4Z_s}$$

Since there are two impedance discontinuities inherent to our definition, SE becomes,

$$SE\ (dB) = 2\left(10 \log \left[\frac{Z_{air}}{4Z_s}\right]\right) + 8.686\ \gamma t$$

or

$$SE\ (dB) = 20 \log \left[\frac{Z_{air}}{4Z_s}\right] + 8.686\ \gamma t\ .$$

The two definitions, thus, yield identical results if P_{TE} (Inc) is considered in the visible region only.

In the case where K_x and K_y are not zero we have an effective contribution from the above integrals over all regions, thus;

$$R\ (dB)_{(\text{loop})} = 2\left(10 \log \frac{Z_{air}}{4Z_s} \left[\frac{\iint_{-\infty}^{+\infty}{}_{-\infty}^{+\infty} \frac{|K_z|}{K_o} |\mathcal{E}_x|^2 \frac{K_y^2}{K_x^2 + K_y^2}\ d K_x\, d K_y}{\iint_{-\infty}^{+\infty}{}_{-\infty}^{+\infty} \frac{|K_z|^2}{K_o^2} |\mathcal{E}_x|^2 \frac{K_y^2}{K_y^2 + K_x^2}\ d K_x\, d K_y}\right]_{\text{all regions}}\right)$$

and from Monroe:

$$R\ (dB) = 20 \log \frac{Z_{wave}}{4\bar{Z}_s}$$

It is thus shown that the definition of shielding effectiveness employed in the Plane Wave Spectrum approach yields results identical to those of HDL-TR-1636 if the discussion is confined to the visible region. Including the contribution of the power of the invisible region provides more accurate results for the shielding effectiveness calculation.

The computer model developed for the investigation calculates the Plane Wave Spectrum of the dipole (and loop) and sums the resulting spectrum with the proper coefficients to produce the incident and transmitted power. Figure 3.6-4 is a graphical representation of the tangential electric field distribution over a plane 12 inches (0.305 M) from a short dipole. The plane wave spectrum of such a distribution is obtained by taking the inverse Fourier transform and is shown pictorially in Figure 3.6-5.

Using the transmitted and incident power, the shielding effectiveness of a 1 mm copper plate was obtained for a loop source, a dipole source, and a uniform plane wave. The results are presented in Figure 3.6-6. The graph shows that shielding effectiveness measurements made with loop antennas will display a much lower value than those measurements made with dipoles. It also shows that shielding effectiveness to EMP is bounded above and below by dipole and loop measurements.

A correction factor can be computed to predict EMP shielding effectiveness from measurements made in the manner of MIL-STD-285: the correction factor is added for loop test (or computed) results while the correction factor is subtracted from the dipole test (or computed) results. Figure 3.6-7 and 3.6-8 show the correction factor (δ) in dB with the difference in the two graphs being due to an apparent difference in antenna spacing. In each case, the dipoles are located symmetrically on either side of the shield (12 inches or 0.305 m). Also, the loops are placed symmetrically 12 inches (0.305 m) on either side of the shield where the spacing is measured to the near edge of the loop. Considering the loop as an incremental loop antenna, the radiating source is 18 inches (0.458 m) from the shield, i.e., the distance to the center of the real loop. Thus, the results of Figure 3.6-7 are considered more appropriate to the MIL-STD-285 situation.

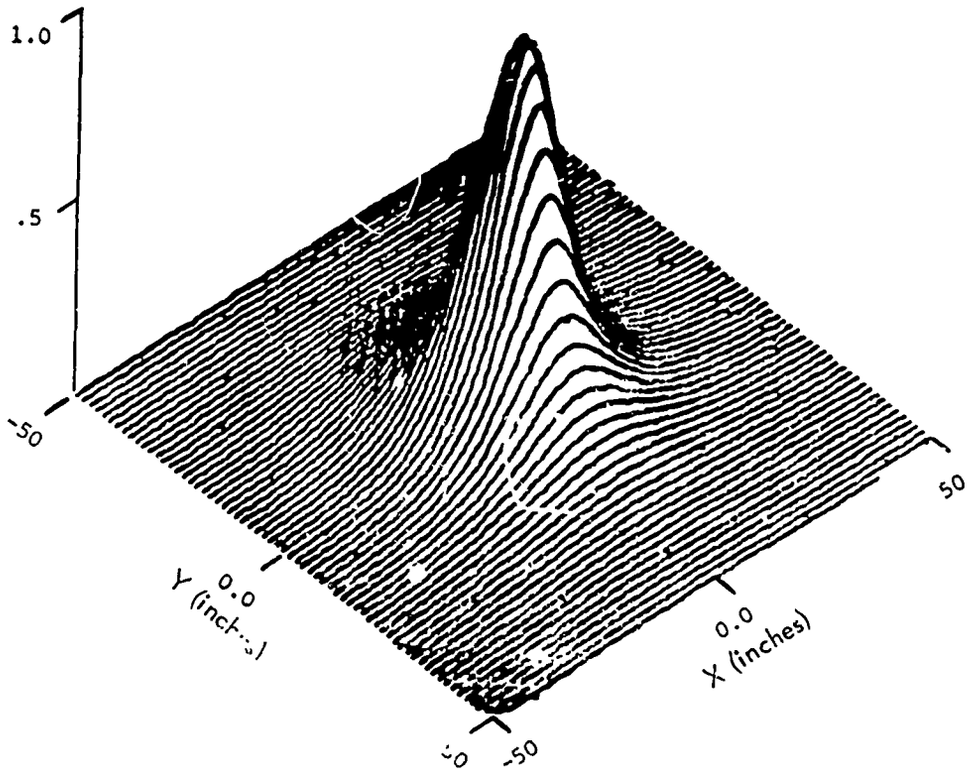

Figure 3.6-4. Normalized Tangential Electric Field Intersecting a Plane at a Distance of 12 Inches from an Elemental Dipole

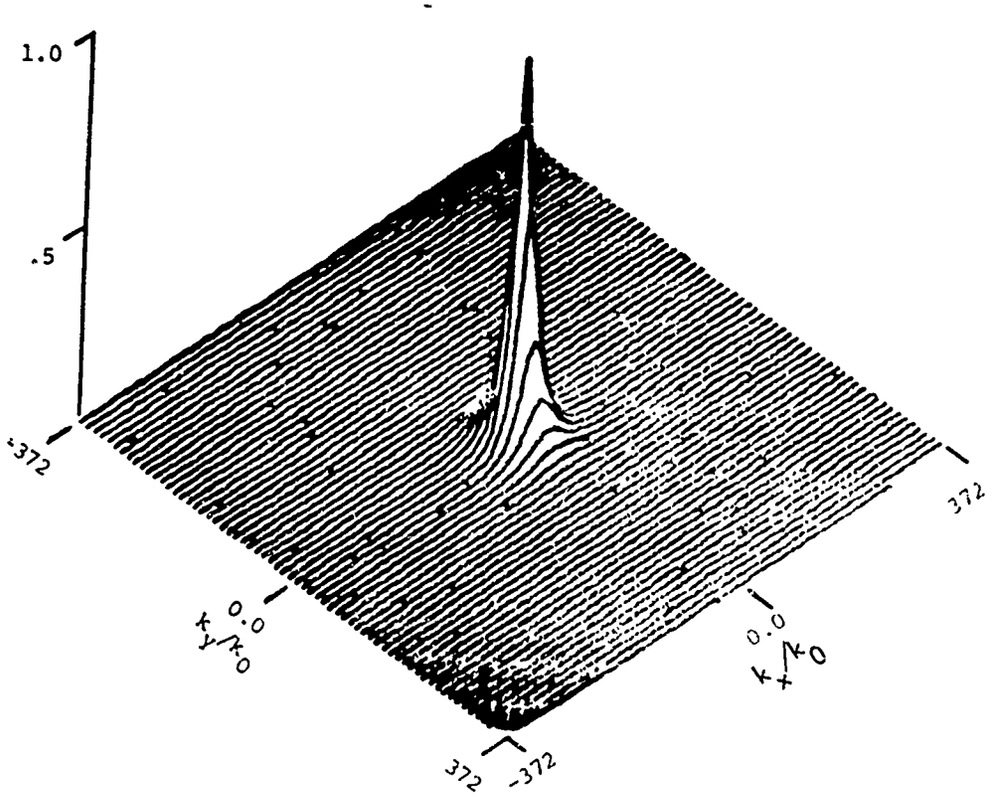

Figure 3.6-5. Normalized Plane Wave Spectrum of the Tangential Electric Field Intersecting a Plane at a Distance of 12 Inches from an Elemental Dipole

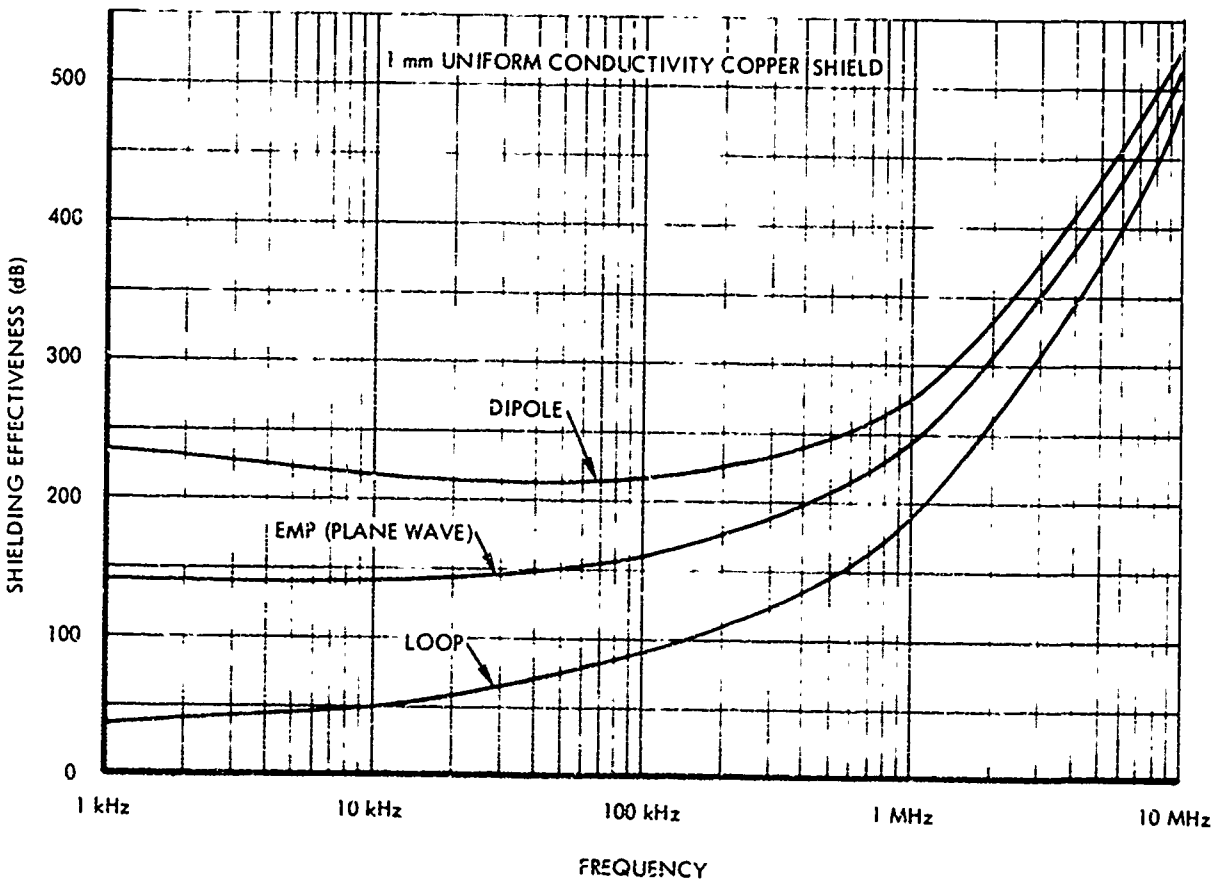

Figure 3.6-6. Shielding Effectiveness Predictions Using the Plane Wave Spectrum Technique in Accordance with MIL-STD-285 Procedures

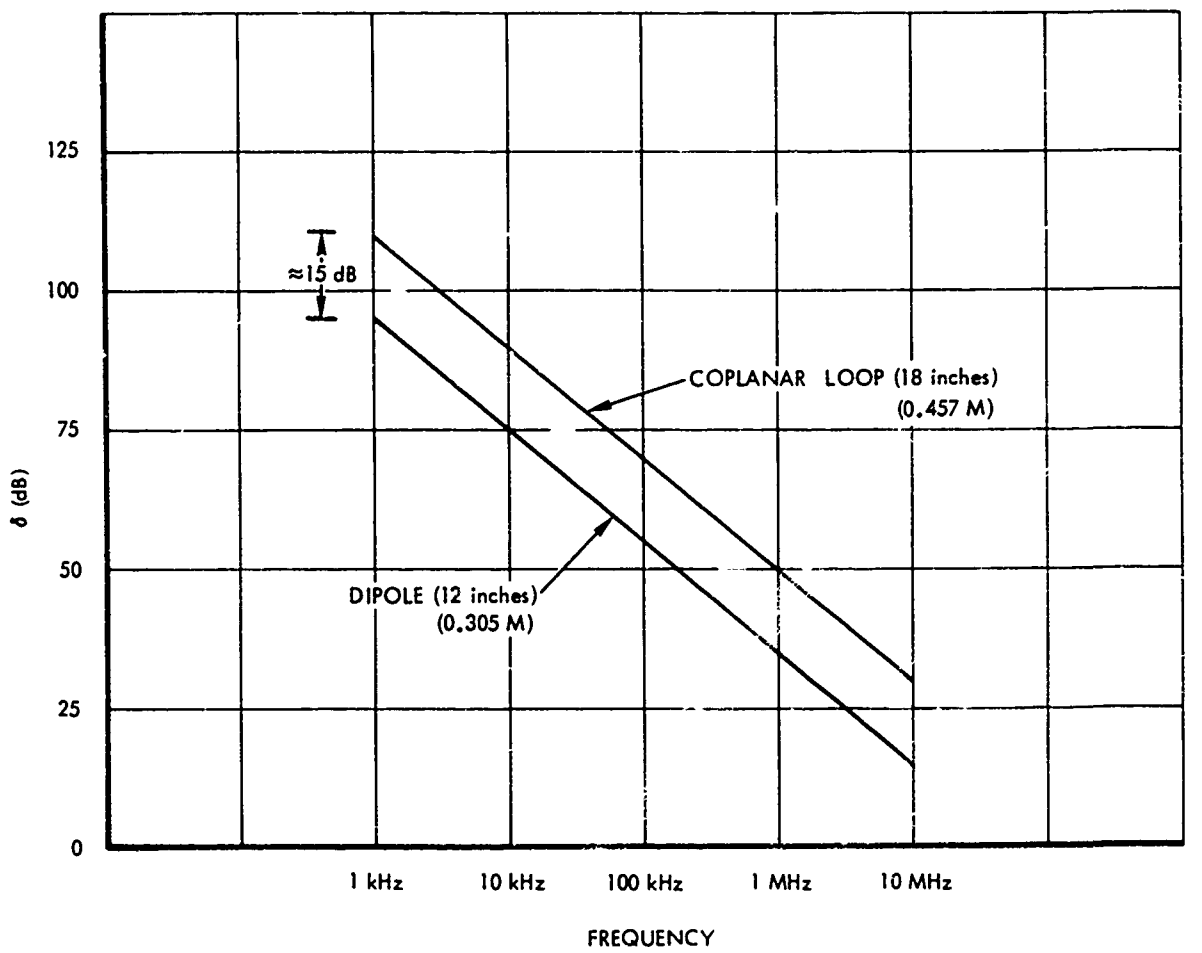

Figure 3.6-7 Plane Wave Spectrum Correction Factor to Compute EMP Shielding Effectiveness from Loop and Dipole Measurements

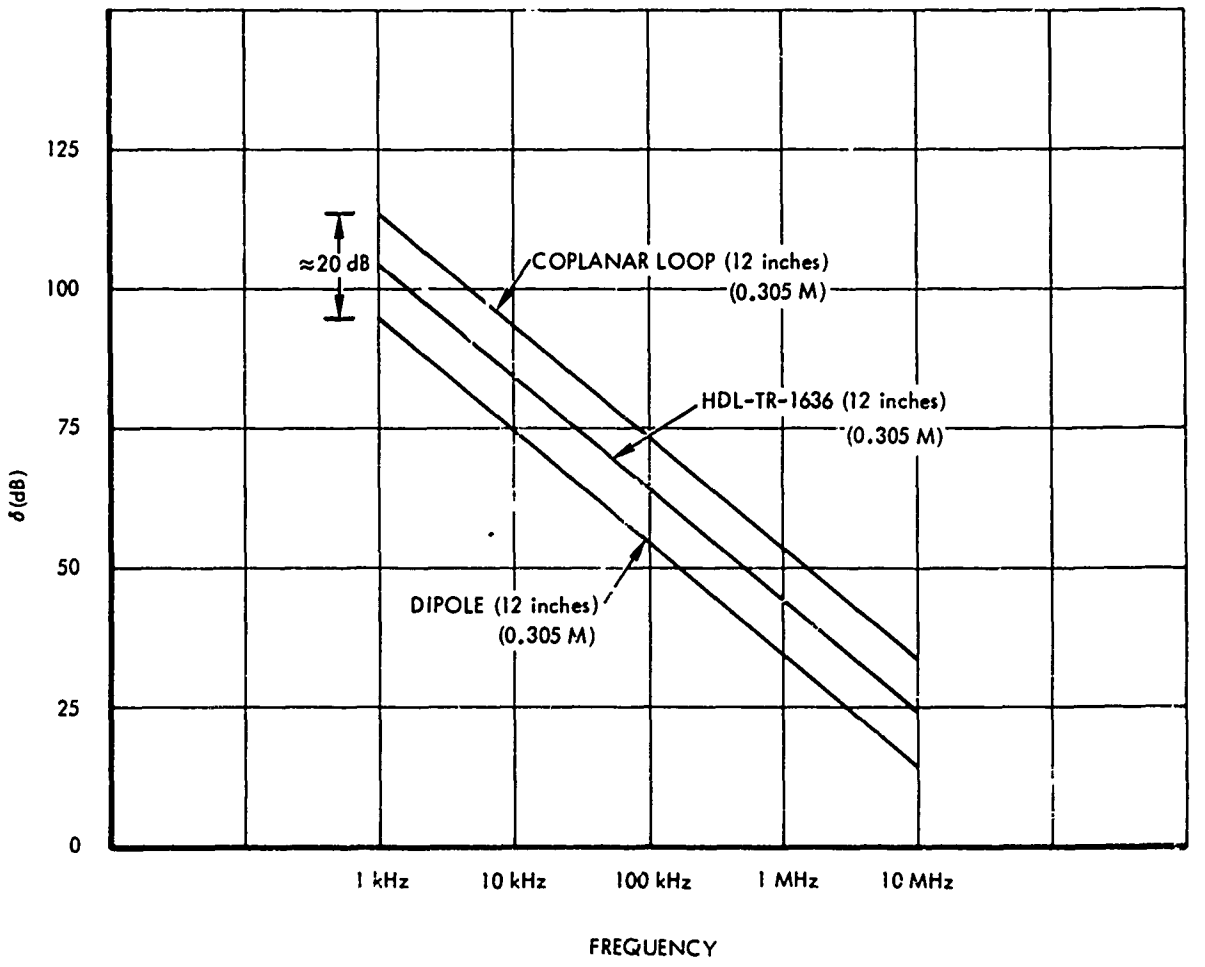

Figure 3.6-8. Plane Wave Spectrum Correction Factor for Coplanar Loop and Dipole Versus HDL-TR-1636 Correction Factor

4.0 CONCLUSIONS

The application of transmission line theory (Schelkunoff approach) in HDL-TR-1636 to the shielding effectiveness problem assumes a plane wave incident on the planar shield. This obviously is not the situation for MIL-STD-285 testing where the shield is located in the extreme near field of the loop and dipole electromagnetic sources. The Plane Wave Spectrum concept is a more rigorous analytical approach since actual loop and dipole near field waveforms are converted to families of plane waves prior to interacting the electromagnetic energy with the planar shield. The calculations are then straightforward applications of plane wave theory to planar surfaces.

The Plane Wave Spectrum technique has been used to provide correction factors for EMP predictions for a uniform conductivity copper shield. While not agreeing precisely with the transmission line technique, these predictions indicate that the HDL-TR-1636 technique is a good engineering approximation for this physical configuration.

We conclude that the Plane Wave Spectrum technique provides a new method for determining the shielding effectiveness of a shield to a plane wave from calculations or measurements made in the manner specified by MIL-STD-285. From a review of the techniques used in the past to calculate shielding effectiveness, the technique is more rigorous and more versatile. Further, the Plane Wave Spectrum technique can be extended to obtain EMP shielding effectiveness predictions of physical three-dimensional structures from measurements made by the methods of MIL-STD-285.

5.0 RECOMMENDATIONS

Further investigation is recommended in the following areas:

1. Validate the current theoretical effort experimentally
   - Provide a suitable planar test bea
   - Employ current generation power sources/amplifiers/antennas/detectors to maximize dynamic range of instrumentation
   - Devise and perform experiments on a uniform conductivity planar shield
2. Extend current CW effort to real, three-dimensional enclosures
   - Revise the theory to address planar shields with penetrations
   - Devise and perform experiments on a planar shield with controlled penetrations to validate theory
   - Provide correction factors between near field and far field shielding effectiveness response of shields containing faults
   - Investigate impact of three-dimensional structures on CW testing - proximity effects of metal on antennas, effects of different environment during calibration and test phases, corner effects, elevation effects, etc.
3. Relate response of shelters to low level CW and specification level pulse signals
   - Investigate saturation effects for ferrous materials
   - Investigate impact on shielding effectiveness of surface currents from external sources (interconnecting cabling)
   - Investigate cavity resonance effects of metallic enclosures resulting from high level electromagnetic pulses.

These investigations should provide a new EMP simulation concept using low level, easily transportable test equipment to augment specification level EMP simulators. Applicability will be to initial acceptance testing, interim test phases and hardness maintenance programs in the field.

REFERENCES

1. Monroe, R., HDL-TR-1636, EMP Shielding Effectiveness and MIL-STD-285 (1973).

2. Anonymous, MIL-STD-285 "Method of Attenuation Measurements for Enclosures, Electromagnetic Shielding, for (sic) Electronic Test Purposes." Department of Defense, 25 June (1956).

3. Schelkunoff, S.A., Electromagentic Waves, Van Nostrand, Princeton, N.J. (1943).

4. Moser, J., IEEE Trans, EMC, Volume EMC-9, page 6 (1967).

5. Jordan, E., Electromagnetic Waves and Radiating Systems, Prentice-Hall, Englewood Cliffs, N.J. (1950).

6. Schelkunoff, S.A. and H.T. Friis, Antenna Theory and Practice, John Wiley and Sons, N.Y. (1952).

7. Booker, H.G. and P.C. Clemmou, Proceeding of IEE, Volume 97, Part III, pages 11-17, 1957.

8. Personal Communication with Professor Giorgia Franceschetti, University of Illinois at Chicago.

9. Adler, R.B., Chou and Fano, Electromagnetic Energy Transmission and Radiation, MIT Press (1968).

10. Proposed IEEE Recommended Practice for Measurement of Shielding Effectiveness of High Performance Shielding Enclosures, Published by IEEE, June 1969.

11. Ficchi, Rocco, F, Electrical Interference, Hayden Book Co., Inc. 1964, p. 32.

DISTRIBUTION LIST

DEPARTMENT OF DEFENSE

Assistant to the Secretary of Defense
Atomic Energy
ATTN: Staff Asst. (R&D)

Director
Defense Advanced Rsch. Proj. Agency
ATTN: Tech. Library
ATTN: AD/E&PS

Director
Defense Civil Preparedness Agency
ATTN: PO(SE)
ATTN: TS AED
ATTN: Admin. Officer
ATTN: RE(EO)

Defense Communication Engineer Center
ATTN: Code R123, Tech. Library
ATTN: Code R400
ATTN: Code R720, C. Stansberry

Director
Defense Communications Agency
ATTN: CCTC/C672
ATTN: Code 930, Monte I. Burgett, Jr.

Defense Documentation Center
12 cy ATTN: TC

Director
Defense Nuclear Agency
ATTN: TISI Archives
ATTN: STVL
ATTN: RAEV
ATTN: RATN
ATTN: VLIS
ATTN: DDST
3 cy ATTN: TITL Tech. Library

Commander
Field Command, Defense Nuclear Agency
ATTN: FCPR
ATTN: FCLMC
ATTN: FCLM

Chief
Livermore Division Fld. Command, DNA
Lawrence Livermore Laboratory
ATTN: FCPRL

National Communications System
ATTN: NCS-TS, Charles D. Bodson

Director
National Security Agency
ATTN: S232
ATTN: R-425, Orlando Van Gunten
ATTN: T412
ATTN: Tech. Library
ATTN: T1213

DEPARTMENT OF DEFENSE (Continued)

OJCS/J-3
ATTN: J-3

Under Secretary of Def. for Rsch. & Engrg.
ATTN: S&SS (OS)
ATTN: G. Barse

DEPARTMENT OF THE ARMY

Project Manager
Army Tactical Data Systems
U.S. Army Electronics Command
ATTN: DRCPM-TDS-BSI

Commander
BMD System Command
ATTN: BMDSC-AOLI

Commander
Harry Diamond Laboratories
ATTN: DRXDO-EM, [illegible] ey
ATTN: DRXDO-TI,
ATTN: DRXDO-TF, k[illegible].d, Jr.
ATTN: DELHD-TD
ATTN: DRXDO-EM-5
ATTN: DRXDO-EM-4
ATTN: DRXDO-RB
ATTN: DELHD-NP
ATTN: DRXDO-EM, Chief, EME Lab.
3 cy ATTN: DRXDO-EM-1
2 cy ATTN: DRXDO-RCC
2 cy ATTN: DRXDO-EM-2
5 cy ATTN: DRXDG-EM-3

Director
U.S. Army Ballistic Research Labs.
ATTN: DRDAR-BLE
ATTN: DRSTE-EL

Commander
U.S. Army COMM-ELEC. Engrg. Instal. Agy.
ATTN: CCC-PRSO-S

Commander
U.S. Army Communications Cmd.
ATTN: CC-OPS-OS
ATTN: CC-OPS-PD

Commander
U.S. Army Communications Cmd.
ATTN: ATSI-CD-MD

Chief
U.S. Army Communications Sys. Agency
ATTN: CCM-RD-T, CCM-AD-SV

Commander
U.S. Army Electronics Command
ATTN: DRSEL-NL-RO, R. Brown
ATTN: DRSEL-GG-TD, W.R. Werk
ATTN: DRSEL-CT-HDK, Abraham E. Cohen

DEPARTMENT OF THE ARMY (Continued)

Division Engineer
ATTN: HNDED-SR

Director
U.S. Army Materiel Sys. Analysis Acty.
ATTN: DRXSY-PO

Commander
U.S. Army Missile Command
ATTN: DRDMI-TRR, Faison P. Gibson
ATTN: DRDMI-EAA
ATTN: DRDMI-TBD
ATTN: DRCPM-PE-EA, Wallace O. Wagner
ATTN: DRCPM-PE-FG, William B. Johnson

Commander
U.S. Army Test And Evaluation Comd.
ATTN: DRSTE-FA

Commander
U.S. Army Training And Doctrine Command
ATTN: ATORI-OP-SW

Commander White Sands Missile Range
ATTN: D.E. Miller
ATTN: TE-AN, Mr. Okuma

DEPARTMENT OF THE NAVY

Commander
Naval Air Systems Command
ATTN: AIR 350F

Commander
Naval Electronic Systems Command
ATTN: PME 117-215

Commander
Naval Ocean Systems Center
ATTN: Code 812, S.W. Lichtman
ATTN: Research Library

Superintendent (Code 1424)
Naval Postgraduate School
ATTN: Code 1424

Director
Naval Research Laboratory
ATTN: Code 2627, Doris R. Folen
ATTN: Code 6624

Officer-In Charge
Naval Surface Weapons Center
ATTN: Code 431, Edwin R. Rathburn
ATTN: Code WR43, L. Libello
ATTN: Code WA51RH, Rm. 130-108

Director
Strategic Systems Project Office
ATTN: NSP-43, Tech. Library
ATTN: SP 2701, John W. Pitsenberger

DEPARTMENT OF THE AIR FORCE

AF Weapons Laboratory, AFSC
ATTN: SUL
ATTN: ELXT
ATTN: NT
ATTN: CA
ATTN: ELP

Commander
Air University
ATTN: AUL/LSE-70-250

Commander
ASD
ATTN: ENFTV

Headquarters
Electronic Systems Division/YS
ATTN: YSEV

Commander, Foreign Te[illegible]vision, AFSC
ATTN: ET[illegible] B.L.[illegible]

Commander
Ogden Air Logistics Center
ATTN: MMEDO, Leo Kidman
ATTN: OO-ALC/MMETH, P.W. Berthel
ATTN: MMEWM

Commander
Rome Air Development Center, AFSC
ATTN: TSLD

SAMSO/IN
ATTN: IND, I.J. Judy

SAMSO/MN
ATTN: MNNH, Capt R.I. Lawrence
ATTN: MNNH, Maj M. Baran

SAMSO/YA
ATTN: YAPC

Commander in Chief, Strategic Air Command
ATTN: SPFS, Maj Brian G. Stephan
ATTN: GARNET F. Matzke
ATTN: DEL
ATTN: NRI-STINFO Library

DEPARTMENT OF ENERGY

University of California
Lawrence Livermore Laboratory
ATTN: Hans Kruger, L-96
ATTN: Terry R. Donich, L-96
ATTN: Librarian
ATTN: Dr. E. Miller

Sandia Laboratories
ATTN: Doc. Con. for Org. 9353, R.L. Parker

OTHER GOVERNMENT AGENCIES

Central Intelligence Agency
ATTN: RD/SI, Rm. 5G48, Hq. Bldg. for OSI/NED/NWB

Administrator
Defense Electric Power Admin.
ATTN: L. O'Neill

Department of Transportation
Federal Aviation Administration
ATTN: Sec. Div. ASE-300

DEPARTMENT OF DEFENSE CONTRACTORS

Aerospace Corporation
ATTN: Irving M. Garfunkel
ATTN: C.B. Pearlston
ATTN: Julian Reinheimer
ATTN: Library

The BDM Corporation
ATTN: Tech. Library

The BDM Corporation
ATTN: Tech. Library
ATTN: J. Schwarz

The Boeing Company
ATTN: B.C. Hanrahan
ATTN: David Kemle
ATTN: D.E. Isbell
ATTN: Kent Tech. Library

Booz-Allen And Hamilton, Inc.
ATTN: Tech. Library
ATTN: Raymond J. Chrisner

Brown Engineering Company, Inc.
ATTN: Fred Leonard

Burroughs Corporation
Federal And Special Systems Group
ATTN: Angelo J. Mauriello

Charles Stark Draper Laboratory, Inc.
ATTN: Kenneth Fertig
ATTN: TIC MS 74

Computer Sciences Corporation
ATTN: Ramona Briggs

Computer Sciences Corporation
ATTN: Alvin T. Schiff

Dikewood Industries, Inc.
ATTN. L. Wayne Davis
ATTN: Tech. Library

EG&G, Inc.
ATTN: C. Giles

General Electric Company
TEMPO-Center for Advanced Studies
ATTN: Royden R. Rutherford
ATTN: DASIAC
ATTN: William McNamara

DEPARTMENT OF DEFENSE CONTRACTORS (Continued)

General Electric Company-TEMPO
ATTN: DASIAC
ATTN: William Alfonte

Georgia Institute of Technology
ATTN: R. Curry

GTE Sylvania, Inc.
Electronics Systems Grp.-Eastern Div.
ATTN: Charles A. Thornhill, Librarian

GTE Sylvania, Inc.
ATTN: J. A. Waldron
ATTN: Charles H. Ramsbottom
ATTN: H & V Group, Mario A Nurefora
ATTN: Comm. Syst. Div., Emil P. Motchok
ATTN: David P. Flood

Harris Corporation
Harris Semiconductor Division
ATTN: V. Pres. & Mgr. Prgms. Div.
ATTN: Eduardo Villaseca
ATTN: Carl Davis
ATTN: William Blackwood
ATTN: William Getson

IIT Research Institute
ATTN: Irving N. Mindel
ATTN: Jack E. Bridges

Institute for Defense Analyses
ATTN: Tech. Info. Ofc.

Intl. Tel. & Telegraph Corporation
ATTN: Tech. Library

IRT Corporation
ATTN: Dennis Swift
ATTN. C.B. Williams

JAYCOR
ATTN: Eric P. Wenaas

JAYCOR
ATTN: Tech. Library

Kaman Sciences Corporation
ATTN: W. Foster Rich
ATTN: Walter E. Ware
ATTN: Jerry I Lubell

Lockheed Missiles & Space Co., Inc.
ATTN: H.E. Thayn
ATTN: Dept 85-85, Samuel I. Taimuty
ATTN: Dept. 81-64, L. Rossi
ATTN: Dept. 81-14, George F. Heath

M.I.T. Lincoln Laboratory
ATTN: Leona Loughlin, Librarian, A-082

Martin Marietta Corporation
ATTN: Mona C. Griffith, Lib. MP-30

McDonnell Douglas Corporation
ATTN: Tom Ender

DEPARTMENT OF DEFENSE CONTRACTORS (Continued)

McDonnell Douglas Corporation
ATTN: Stanley Schneider
ATTN: Tech. Library Services

Mission Research Corporation
ATTN: William C. Hart
ATTN: Emp. Group

Mission Research Corporation
ATTN: L.N. McCormick

Mission Research Corporation
ATTN: V.A.J. Van Lint

The Mitre Corporation
ATTN: Theodore Jarvis
ATTN: M.E. Fitzgerald

R & D Associates
ATTN: Richard R. Schaefer
ATTN: Leonard Schlessinger
ATTN: Doc. Con
ATTN: Charles Mo
ATTN: B. Gage
ATTN: J. Bombardt

The Rand Corporation
ATTN: LIB-D

Raytheon Compa[illegible]
ATTN: [illegible]man H. Joshi, Radar Sys. Lab.

DEPARTMENT OF DEFENSE CONTRACTORS (Continued)

Raytheon Company
ATTN: Harold L. Flescher

Science Applications, Inc.
ATTN. Frederick M. Tesche

Science Applications, Inc.
ATTN: R. Parkinson

Science Applications, Inc.
ATTN: William L. Chadsey

Sidney Frankel & Associates
ATTN: Sidney Frankel

Spire Corporation
ATTN: Roger G. Little

SRI International
ATTN: Arthur Lee Whitson

SRI International
ATTN: Mr. Hullings

Texas Tech. University
ATTN: Travis L. Simpson

TRW Defense & Space Sys. Group
ATTN: O.E. Adams, R1-1144
ATTN: L.R. Magnoiia